

AALBORG UNIVERSITY ESBJERG

---

# Design of an Impeller for a Centrifugal Pump

---

B.Sc. Project: Thermo Mechanical Energy Systems

EN6TP-1-F16

9/6/2016



**Institute of Energy Technology**

Niels Bohrs Vej 8

DK-6700 Esbjerg

<http://www.en.esbjerg.aau.dk>

**Abstract:****Title:**

Design of an Impeller for a Centrifugal Pump

**Theme:**

Thermo Mechanical Energy Systems

**Project period:**

Spring Semester 2016

**Project group:**

EN6TP-1-F16

**Members:**

Jensen, Rune Kjerrumgaard  
Lassen, Kasper Lindgren

**Supervisor:**

Mandø, Matthias

**No. printed Copies:** 2

**No. of Pages:** 60

**No. of Appendix Pages:** 13

**Total no. of pages:** 73

**Completed:** 9/6/2016

The subject of this report is to design an impeller for a centrifugal pump for a specific operation point. The centrifugal pump will be investigated with primary focus on the impeller. The pump performance curve is explained as the designed impeller will be tested on an existing pump test stand at Aalborg University Esbjerg. To see how the blade and fluid velocity is behaving ideally throughout the impeller, the velocity triangles is investigated. The losses will be explained as different mechanical and hydraulic losses in the impeller and volute, makes the ideal behavior not attainable.

Two different calculation models by Willi Bohl and Johann Gülich is used to design impellers for a specific operation point. The two impellers will be compared with an existing impeller by Grundfos. The impellers was drawn in Inventor and constructed by a 3D printer. The tests showed that the impeller designed with Gülich had a pump curve that was very reminiscent of the Grundfos impeller. The pump curve of the Bohl impeller was at a constantly lower head than both the Grundfos and Gülich impellers. Therefore the impeller proposed by Gülich creates an impeller closer both in operation and dimensions to the Grundfos impeller compared to Bohl.



## GROUP MEMBERS

---

Jensen, Rune Kjerrumgaard

rkje13@student.aau.dk

---

Lassen, Kasper Lindgren

klla13@student.aau.dk

## CONTENTS

<b>1. Introduction</b>	<b>1</b>
1.1. Goals and Contents of the Report . . . . .	2
<b>2. Problem Analysis</b>	<b>3</b>
2.1. Testing Stand . . . . .	3
2.2. Centrifugal Pump . . . . .	4
2.2.1. The Impeller . . . . .	5
2.3. Performance Curves . . . . .	8
2.3.1. Pump Pressure . . . . .	8
2.3.2. Head . . . . .	9
2.3.3. Efficiency . . . . .	9
2.4. Velocity Triangles . . . . .	10
2.4.1. Inlet . . . . .	11
2.4.2. Outlet . . . . .	11
2.5. Power Transfer . . . . .	12
<b>3. Pump Losses</b>	<b>13</b>
3.1. Mechanical Losses . . . . .	14
3.2. Flow Friction . . . . .	14
3.3. Contraction and Expansion . . . . .	15
3.4. Recirculation Losses . . . . .	16
3.5. Disk Friction . . . . .	16
3.6. Leakage . . . . .	17
3.7. Summary . . . . .	18
<b>4. Impeller design</b>	<b>19</b>
4.1. Willi Bohl Calculation Model . . . . .	20
4.1.1. Impeller Outer Diameter . . . . .	20
4.1.2. Blade Inlet Height and Outlet Angle . . . . .	21
4.1.3. Blade Inlet Angle . . . . .	23
4.1.4. Number of Blades . . . . .	23
4.1.5. Blade Outlet Height . . . . .	24
4.2. Johann F. GÜLICH Calculation Model . . . . .	25
4.2.1. Impeller Outer Diameter . . . . .	25
4.2.2. Number of Blades and Outlet Blade Angle . . . . .	26
4.2.3. Blade Outlet Height and Blade Inlet Angle . . . . .	28
4.3. Impeller Comparison . . . . .	29
<b>5. Impeller Construction</b>	<b>31</b>
5.1. Meridional Section . . . . .	31
5.2. Blade Construction . . . . .	34
5.3. Cross Sectional Vane Area . . . . .	37

<b>6. Test of Impellers</b>	<b>40</b>
6.1. Grundfos Impeller . . . . .	41
6.2. Willi Bohl Impeller Design . . . . .	42
6.3. Johann GÜLICH Impeller Design . . . . .	44
6.4. Summary . . . . .	45
<b>7. Discussion</b>	<b>46</b>
<b>8. Conclusion</b>	<b>49</b>
<b>Appendix</b>	<b>51</b>
A. Curriculum . . . . .	51
B. Willy Bohl MATLAB Script . . . . .	52
C. Johann GÜLICH MATLAB Script . . . . .	54
D. Blade Design MATLAB Script . . . . .	56
E. Bohl Constrution Sketches . . . . .	60
F. Impeller Test 2 Graphs . . . . .	61
G. CD Content . . . . .	63

## NOMENCLATURE

Symbol	Definition	Unit
$A$	Area	$m^2$
$a$	Width between impeller blades	$m$
$b$	Blade height or meridional section width	$m$
$c \& V$	Meridional velocity	$m/s$
$D \& d$	Diameter	$m$
$e \& s$	Impeller blade thickness	$m$
$g$	Gravitational acceleration	$m/s^2$
$H$	Head	$m$
$h$	Height	$m$
$i$	Incidence	$^\circ$
$k$	Dimensionless parameter	—
$m$	Mass	$kg$
$n$	Rotational speed	$rpm$
$n$	Number of readings	—
$n_q$	Specific speed	—
$P$	Pressure	$Pa$
$Q$	Volumetric flow rate	$m^3/s$
$R_{sch}$	Radius of circular arc blade	$m$
$r$	Radius	$m$
$U \& u$	Tangential velocity of impeller	$m/s$
$v$	Velocity	$m/s$
$W$	Power	$W$
$W \& w$	Relative velocity	$m/s$
$x$	Observation	—
$Y$	Specific work	$m^2/s^2$
$z$	Number of blades	—

Symbol	Definition	Unit
$\alpha$	Angle between relative and tangential velocity	°
$\beta$	Blade angle	°
$\Delta$	Change	—
$\epsilon_{lim}$	Dimensionless parameter	—
$\eta$	Efficiency	%
$\gamma$	Slip factor	—
$\lambda$	Angle between vanes and side disks	°
$\omega$	Angular velocity	rad/s
$\Psi$	Head coefficient	—
$\rho$	Density	kg/m <sup>3</sup>
$\tau$	Blade blockage factor	—
$\tau$	Torque	Nm
$\zeta$	Dimensionless loss coefficient	—

Subscripts & Subscripts	Definition
.	Rate
*	Dimensionless
—	Arithmetic mean
<i>a</i>	Outer impeller
<i>avg</i>	Average
<i>b</i>	Arithmetic average
<i>B</i>	Blade
<i>dyn</i>	Dynamic
<i>hyd</i>	Hydraulic
<i>i</i>	Inner stream line
<i>i</i>	Observation number
<i>k</i>	Cross sectional
<i>La</i>	Impeller
<i>m</i>	Meridional & Mean stream line
<i>n</i>	Hub
<i>r</i>	Radial
<i>s</i>	Inner
<i>stat</i>	Static
$\Theta$	Tangential component



## 1. INTRODUCTION

A pump is a flow machine that is used to move a fluid by mechanical power. The fluid flowing through a centrifugal pump is exposed to a pressure difference between the inlet and outlet of the pump when in operation.

The most significant component in the centrifugal pump, concerning the pressure difference and flow characteristics, is the impeller. There are many different pump and impeller types for different applications, such as single stage and multi-stage pumps and axial, semi-axial and radial impellers.

An existing pump test stand is available at the flow lab at Aalborg University Esbjerg where it is possible to change the impeller for performance tests.

The problem analysis will focus on the characteristics of the different radial impeller design parameters, but it will also contain an explanation of the centrifugal pump components and their functioning. This combined with the basic formulas and ideas behind a pump standard curve should create a good basis for understanding what is needed to be taken into consideration when designing an impeller for a specific operation point.

The design point will be chosen to be the same as the existing Grundfos pump's so as to be able to compare it with two different impellers developed from two different design guides. As the pump test stand is designed for radial impellers, the impellers will also be radial for the volute to function properly.

Normally when producing impellers, moulds have to be developed which is an expensive and time consuming process therefore the impellers designed in this study will be drawn and designed in Autodesk Inventor so as to be able to 3D print them for testing.

This B.Sc. project was written from the 1<sup>st</sup> of February to the 9<sup>th</sup> of June 2016 by the study group EN6TP-1-F16 comprising of Kasper Lindgren Lassen and Rune Kjerrumgaard Jensen. The report is structured in accordance with the B.Sc. project guidelines, in collaboration with supervisor Matthias Mandø from the Department of Energy Technology at Aalborg University Esbjerg.

### 1.1. GOALS AND CONTENTS OF THE REPORT

The goals and contents below have been made to comply with the curriculum of the bachelor project, which can be found in App. A.

1. To gain an understanding of a centrifugal pump.
2. To describe different impeller types and choose a specific type for a given case.
3. To create a mathematical model of an impeller for an existing pump setup.
4. To design a 3D-CAD model of an impeller for specific operation point.
5. To manufacture a prototype.
6. To test the original Grundfos and 3D printed impellers in an experimental setup and determine their pump curves.

In the experimental pump test setup at AAUE the pump NK32-125/142, designed by Grundfos, is currently present with a specific impeller type which is designed at a nominal point with a lifting height of  $23.4m$  and a flow rate of  $28m^3/h$ .

Two different design guides suggested by "Strömungsmaschinen 2" and "Centrifugal Pumps" written by Willy Bohl and Johann Friedrich Gülich respectively were used to design impellers that had the same operation point as the original Grundfos impeller. Because all three impellers have the same operation point it is possible to see how their differences influenced their performance curve.

This problem should allow for both gaining experience with experimental work and analyzation of the results for comparison with the expected results of the design guides which were one of the more important skills in the curriculum. Furthermore it will be investigated whether it is possible to 3D print the impeller since this could reduce time and eliminate expensive moulds.

An additional learning goal is gaining experience with:

- Inventor 3D-CAD drawing software.

Inventor will be used for drawing the 3D sketch of the impeller and will therefore be crucial for the project.

## 2. PROBLEM ANALYSIS

This section will clarify the components in the existing pump testing stand at AAUE and their functioning. An explanation of a pump performance curve will be included so that it is clear what parameters influence the choice of pump for a specific operation point. The centrifugal pump will also be investigated as well as different types of impellers.

### 2.1. TESTING STAND

The testing of the designed impellers were conducted on an already existing pump test stand, illustrated in Fig. 1, constructed in accordance with the International Standard ISO 9906.

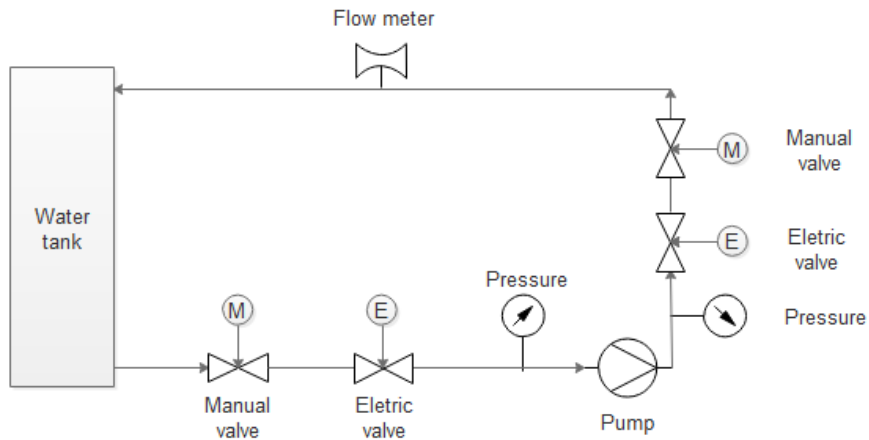


Figure 1: Picture of the pumping stand at AAUE.

The setup consists of a Grundfos NK32-125/142 2-pole centrifugal pump, which has the following specifications:

Symbol	Definition	Value
$W$	Power	3000W
$n$	Rotational speed	2900rpm
$Q$	Design flow rate	$28m^3/h$
$H$	Design head	23.4m

Table 1: Pump specification for Grundfos NK32-125/142.

A round stainless steel water tank with a height of 1500mm and a volume of 287L is connected to the pump, as seen on Fig. 1. A thermometer is mounted at the bottom of the tank to measure the water temperature.

For calculation of the head, pressure is measured at the inlet and the outlet of the pump with Danfoss MBS 33 pressure transmitters.

For flow measurements an Isomag MS 2500 flowmeter is used. The flowmeter is placed after the pump, and has a diameter of 40mm. The range in which the Isomag flowmeter has an instrumental uncertainty of  $\pm 1.5\%$  is within a flow rate range of  $0.75m^3/h < Q < 45m^3/h$ .

Two electronically controlled valves are installed in the testing stand. One is placed after the pump to change the water flow and one before the pump for NPSH tests. The valves are from Belimo and are able to provide position feedback. A control station is placed at the end of the pumping stand. All electronic measuring components are connected, managed and processed here. After the data has been processed it will be transmitted to a USB-key with a myRIO.[1]

## 2.2. CENTRIFUGAL PUMP

This section will cover the mechanical parts of the pump in the test stand and the components' basic functionality. The pump in the test stand is a single stage centrifugal pump designed for radial impellers. Its mechanical components are sketched in Fig. 2.

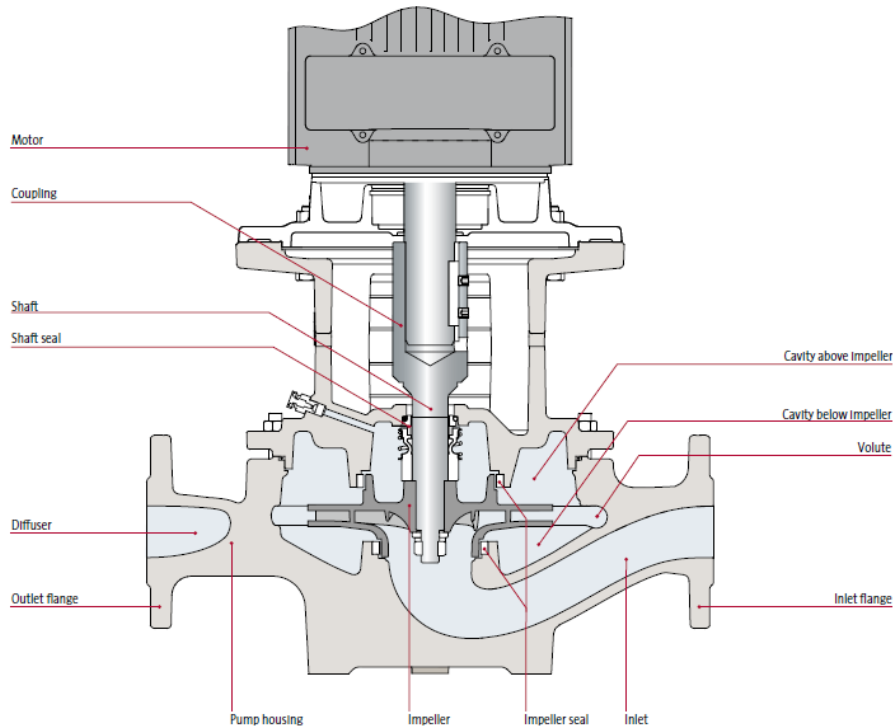


Figure 2: Mechanical parts in a single stage centrifugal pump.[2]

The pump has three main components: Motor, pump housing and within the pump housing an impeller. The motor, which actuate the pump, is connected to the impeller by a coupling and a shaft. When the pump is active, the motor will force the impeller to rotate, which in turn, will force the fluid to flow from the inlet to the outlet by the pressure difference created in the fluid over the impeller. The pump housing's function is to collect the fluid that exits the impeller. To do this efficiently, the pump housing is often shaped as a volute for a radial pump, which is also the case for the pump in the test stand. This pressure difference across the pump is not solely dependent on the impeller, but also on the inner shape and dimensions of the pump housing, but to a lesser extent.

#### 2.2.1. THE IMPELLER

The impeller is the active component in the pump housing and has great effect on the pumps efficiency and working area. Therefore it is important to determine what speaks for and against the different impeller types as well as the different blade orientations within the impeller.

The radial impeller works by the fluid being sucked into the pump eye and exiting in the radial direction of the impeller. The suction is created as the impeller via its blades is forcing the fluid to flow when it is rotating. An illustration of the flow in the impeller and of the impeller blades are seen in Fig. 3.

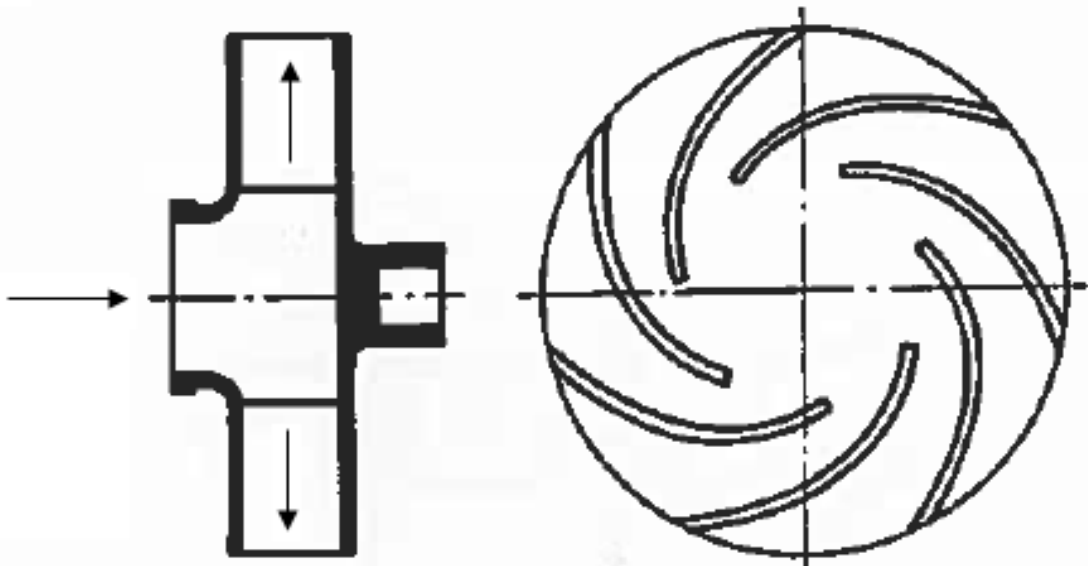


Figure 3: Flow in a radial impeller and sketch of impeller.[3]

The radial impeller blades are attached to a back plate, called the shroud, when this is the only attachment the impeller is described as open. If there is also attached a plate on the top of the blades it is described as closed. The open radial impeller is usually preferred in applications where the working fluid contains larger particles, as is the case

with sewerage pumps. A disadvantage of the open impeller is that there can be an occurrence of back flow which decrease the pump efficiency. Therefore closed impellers are preferred when working with clear water, as it does not contain large particles.[3] Three different blade orientation angles are illustrated in Fig. 4 where  $\beta_1$  is the blade inlet angle and  $\beta_2$  is the blade outlet angle. The blade outlet angle can only have three different orientations:

**Forward**  $\beta_2 > 90^\circ$

**Radial**  $\beta_2 = 90^\circ$

**Backward**  $\beta_2 < 90^\circ$

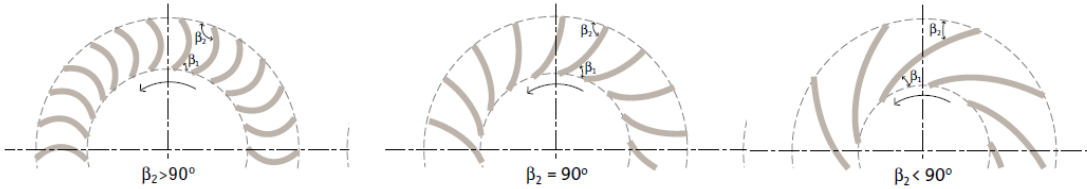


Figure 4: The three different blade orientation angles.[2]

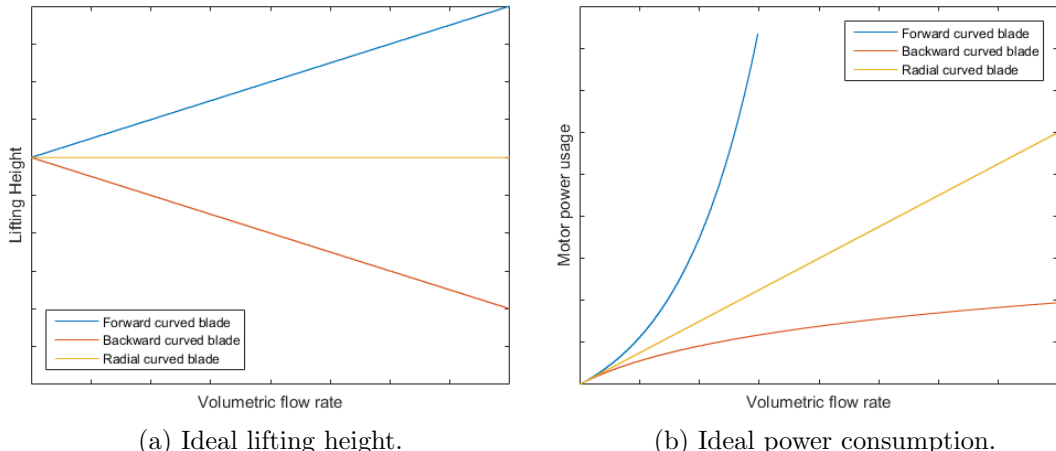


Figure 5

In Fig. 5a and 5b the theoretical lifting height and power usage of the pump is illustrated. The forward curved blade will cause the lifting height to increase with increasing flow rate which will cause the pump shaft requirement to increase exponentially which would not be feasible as big motors would be required. The radial curved blade will have a constant lifting height and is therefore independent of the volume flow which means that the pump shaft power requirement would increase linearly which will also not be feasible for the same reasons as with the forward curved blades. The backward

curved blades would cause the lifting height to decrease with increasing flow rate which would cause the pump shaft power requirement to still increase to a lesser extent than the other two blade orientations. Therefore it is advantageous to design the backward curved blade orientation from the perspective of not needing a big motor when working outside the operation point.

Inside the pump housing the diameter of the impeller can differ to be able to get a lower lifting height, as illustrated in Fig. 6.

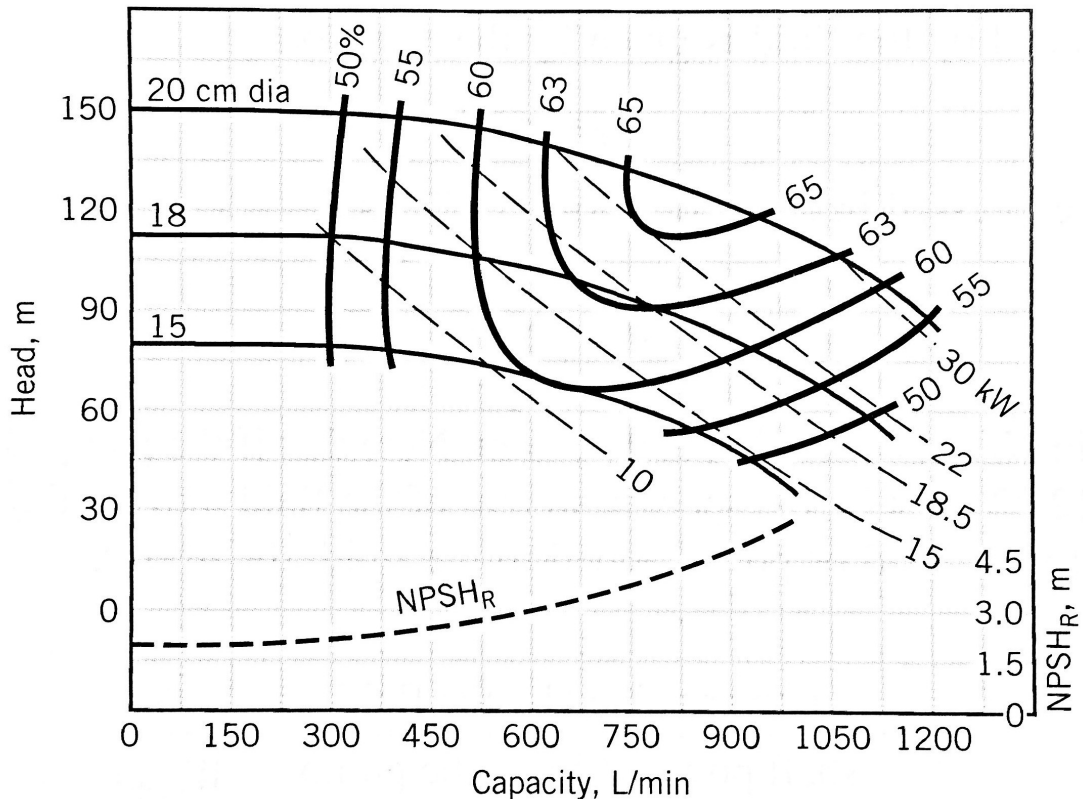


Figure 6: Performance curve for three different impeller diameters.[4]

It can be concluded that the smaller the impeller diameter the smaller the lifting height. Another very important thing to notice is that the smaller the pump diameter the smaller the efficiency for impellers with identical geometry.

### 2.3. PERFORMANCE CURVES

The pump performance curve is used to predict the pump performance under different operation conditions e.g. how the flow rate effects the head.

A standard curve consists of both a head and an efficiency curve as a function of the flow rate. The combination of the head and efficiency curves makes it possible to determine if the pump is useful or efficient at the desired operation point. The power consumption and the NPSH of the pump are also often illustrated in addition to the standard curve. Both diagrams are illustrated in Fig. 7.

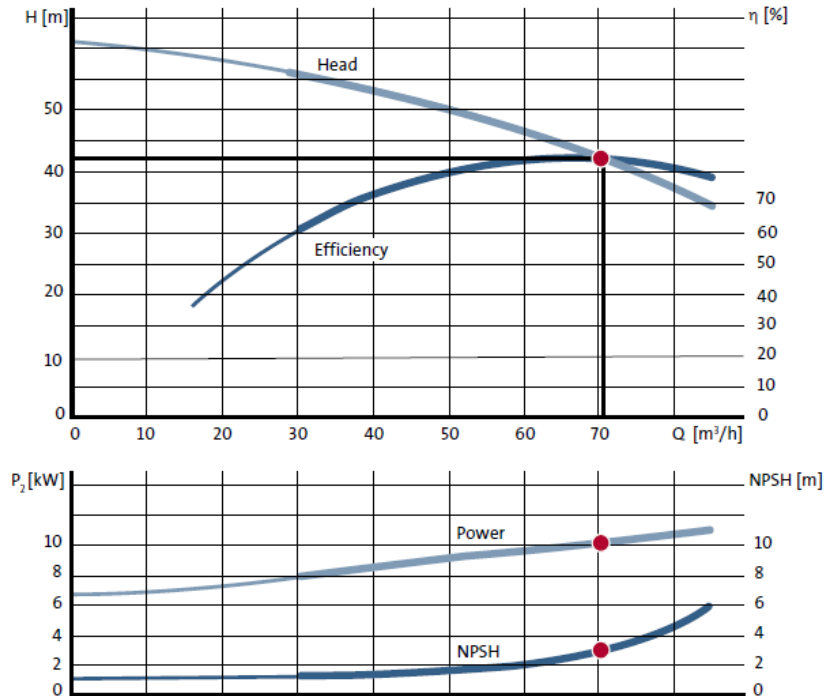


Figure 7: Standard pump curve with power and NPSH.[2]

The pump curves describes the operation of the complete pump i.e. the pressure difference is measured before and after the pump and the efficiency is a measure of the power consumption contra the energy transferred to the working fluid.

#### 2.3.1. PUMP PRESSURE

The differential pressure across the pump is the sum of the static, dynamic and hydrostatic pressure, as in Eq. (1).

$$\Delta P_{total} = \Delta P_{stat} + \Delta P_{dyn} + \Delta P_{hyd} \quad (1)$$

Here the  $\Delta P_{stat}$  is the static pressure difference measured between the inlet and outlet of the pump and is defined as in Eq. (2).

$$\Delta P_{stat} = \Delta P_{stat,out} - \Delta P_{stat,in} \quad (2)$$

The  $\Delta P_{dyn}$  is the dynamic pressure differential which is depended on the velocity change between inlet and outlet of the pump and is calculated by Eq. (3).

$$\Delta P_{dyn} = \frac{1}{2} \rho (v_{out}^2 - v_{in}^2) \quad (3)$$

Here  $v$  is the flow velocity and  $\rho$  is the density of the fluid. It is important to include the dynamic pressure difference if the pipe diameter changes between the inlet and outlet of the pump.

$\Delta P_{hyd}$  is the hydrostatic pressure difference and is dependent on the vertical position between the pressure gauge connected before and after the pump and is described as potential energy in Eq. (4).

$$\Delta P_{hyd} = h \rho g \quad (4)$$

Where  $h$  is the height.

### 2.3.2. HEAD

The QH curve seen in Fig. 7 is a relation between head and volumetric flow rate produced by the pump. When the valve after the pump is completely closed, the flow rate is zero and the highest head is obtained i.e. the cut off head. By gradually opening the valve a higher flow rate would be obtained at the cost of head as the pressure difference across the pump will decrease. The relation between them can be seen in Eq. (5).

$$H = \frac{\Delta P_{total}}{\rho g} \quad (5)$$

Here  $\rho$  is the density of the water through the pump,  $\Delta P_{total}$  is the differential pressure and  $g$  is the gravitational acceleration.

### 2.3.3. EFFICIENCY

The hydraulic power is the power transferred from the impeller shaft to the fluid. The hydraulic power,  $W_{hyd}$ , seen in Eq. 6 is always less than the power supplied because of the loss in the motor and pump. The total efficiency,  $\eta_{tot}$ , is the ratio between the hydraulic power and the power supplied to the motor,  $W_1$ , as in Eq. 7.

$$W_{hyd} = \Delta P_{hyd} Q \quad (6)$$

$$\eta_{tot} = \frac{W_{hyd}}{W_1} \quad (7)$$

The best efficiency point is the point at which the pump has been designed and therefore where it reaches its highest efficiency. In Fig. 7 the best efficiency point is marked with red dots and the operation point should be as close as possible to this point when choosing a pump.[2]

## 2.4. VELOCITY TRIANGLES

The pump performance can be evaluated by fundamental methods. When energy is transferred to the shaft in the form of mechanical energy, the impeller convert the energy to a static pressure and a velocity increase of the working fluid.

The pump performance can be described through flow velocity triangles at the inlet and outlet of the impeller in the means of impeller diameters and rotational speed. Velocity triangles describes the flow of the water streams by its magnitude and direction. For an impeller with backward curved blades the velocity triangles is illustrated are Fig. 8.

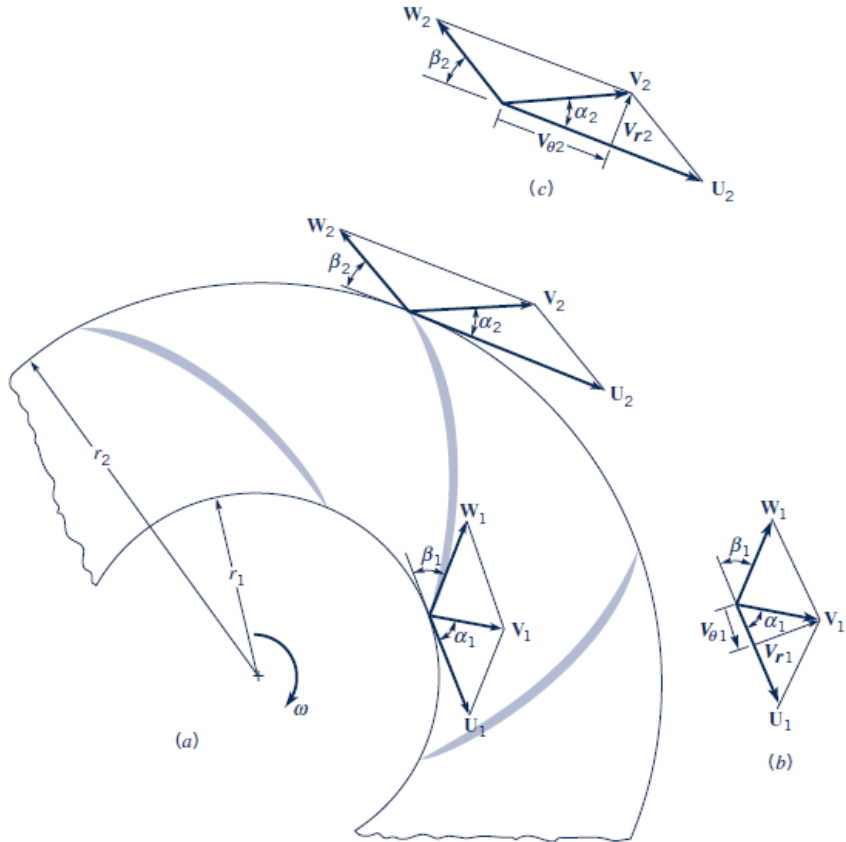


Figure 8: Velocity triangles at the inlet and outlet of the impeller.[4]

$W$  is the relative velocity to the rotating impeller,  $U$  is the tangential velocity and  $V$  is the absolute velocity to the surroundings. The angle  $\alpha$  is the angle between the tangential blade velocity and the absolute velocity and  $\beta$  is the angle between the relative velocity and the tangential velocity of the blade.  $\beta$  is also defined as the blade angle.

As seen on Fig. 8 the velocity triangles is drawn at both the inlet and outlet of the impeller, by these the pump performance can be calculated with Euler's pump equation, Eq. 20. An illustration of the meridional section of the impeller is seen in Fig. 9.

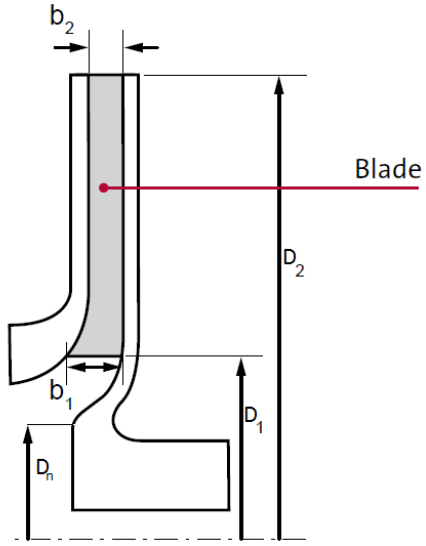


Figure 9: A radial impeller seen from the side.[2]

#### 2.4.1. INLET

Normally the angle  $\alpha_1$  is considered  $90^\circ$  which means the blades are perpendicular to the tangential direction.

The suction area of the impeller is calculated with Eq. (8)[5].

$$A_1 = \frac{\pi}{4}(D_1^2 - D_n^2) \quad (8)$$

The absolute velocity of the fluid at the inlet,  $V_1$ , also called meridional velocity, is calculated by Eq. (9):

$$V_1 = \frac{Q_{impeller}}{A_1} \quad (9)$$

and the inlet tangential velocity of the blades,  $U_1$ , is calculated with Eq. (10).

$$U_1 = 2\pi r_1 \frac{n}{60} \quad (10)$$

Where  $n$  is the rotational speed in rpm.

By Eq. (9) and (10) the blade inlet angle  $\beta_1$  can be found with Eq. (11).

$$\tan\beta_1 = \frac{V_1}{U_1} \quad (11)$$

#### 2.4.2. OUTLET

The outlet area of the radial impeller can be calculated with Eq. (12):

$$A_2 = 2\pi r_2 b_2 \quad (12)$$

The meridional and tangential outlet velocity is calculated in a similar manner as for the inlet velocity triangle.[2]

To find the relative velocity,  $W_2$ , the tangential velocity of the absolute velocity,  $V_{\Theta 2}$ , and the blade outlet angle,  $\beta_2$ , is used:

$$W_2 = \frac{V_{\Theta 2}}{\sin \beta_2} \quad (13)$$

$$\cot \beta_2 = \frac{U_2 - V_{\Theta 2}}{V_{r2}} \quad (14)$$

The flow rate can be calculated by Eq. (15) [4].

$$Q = 2\pi r_2 b_2 V_{\theta 2} \quad (15)$$

## 2.5. POWER TRANSFER

The power or torque transferred from the shaft to the fluid flowing through the impeller changes the fluid velocity.

The torque delivered to the fluid is described by the Euler turbomachine equation as in Eq. (16).

$$\tau = \dot{m}(r_2 V_{\theta 2} - r_1 V_{\theta 1}) \quad (16)$$

To transfer the torque to shaft mechanical power, the torque is multiplied by the angular velocity as seen in Eq. (17)

$$W_{shaft} = \dot{m}(\omega r_2 V_{\theta 2} - \omega r_1 V_{\theta 1}) \quad (17)$$

As the mass flow through the impeller is equal to the density multiplied by the fluid flow rate and the angular velocity multiplied by the radius equals the tangential velocity, Eq. (17) yields Eq. 18.

$$W_{shaft} = Q\rho(U_2 V_{\theta 2} - U_1 V_{\theta 1}) \quad (18)$$

Eq. (18) describes the power supplied from the shaft to the fluid.[6]

To transfer the shaft power to power per unit Eq. (19) is used.

$$w_{shaft} = \frac{W_{shaft}}{\rho Q} = U_2 V_{\theta 2} - U_1 V_{\theta 1} \quad (19)$$

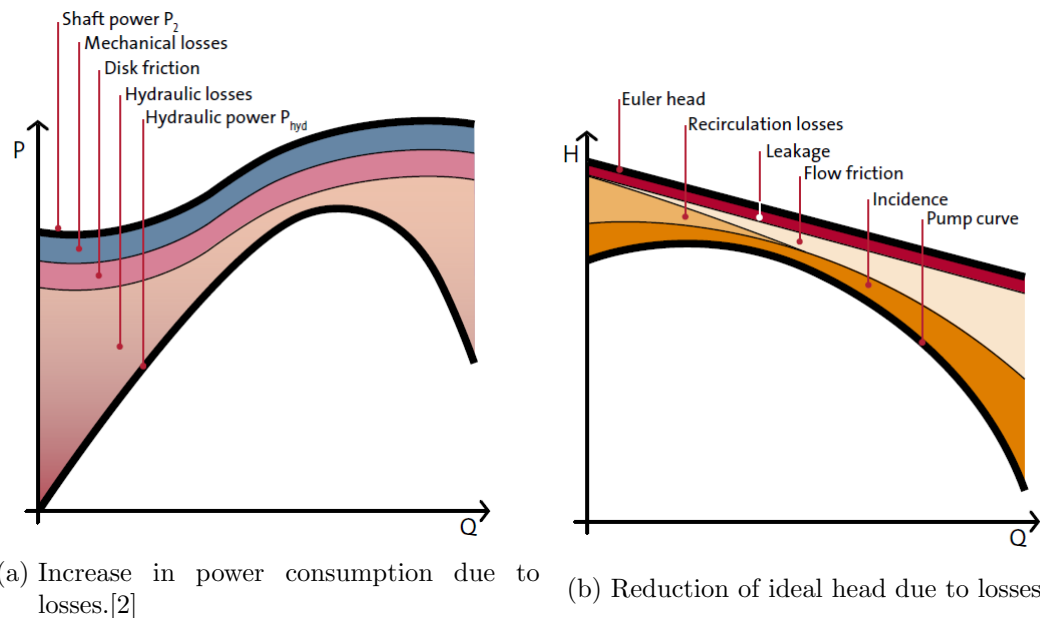
The ideal head can be calculated by combination of the hydraulic pressure, Eq. 4, and the outlet pressure of the pump and is expressed as the Euler's pump equation, in Eq. 20.

$$H = \frac{U_2 V_{\theta 2} - U_1 V_{\theta 1}}{g} \quad (20)$$

In an ideal case the hydraulic power is equal to the mechanical power, as in Eq. 20, but because of several mechanical and hydraulic losses this is not attainable and a decrease in the pump performance is therefore expected.[4]

### 3. PUMP LOSSES

If the Euler turbomachine equation as explained in Sec. 2.3.3 is equal to the hydraulic power, the impeller performance is assumed loss free. In reality the pump performance is lower due to several mechanical and hydraulic losses in the pump casing and impeller. The losses causes a higher power consumption (Fig. 10a) and a smaller head (Fig. 10b) and thereby a lower efficiency.



(a) Increase in power consumption due to losses.[2]

(b) Reduction of ideal head due to losses.[2]

Figure 10

On Fig. 11 the different components which causes the hydraulic and mechanical losses involving volute, diffuser, inner and outer impeller surface, front cavity seal, inlet, bearing and shaft seal.[2]

The different impeller and pump casing losses will be described throughout this section.

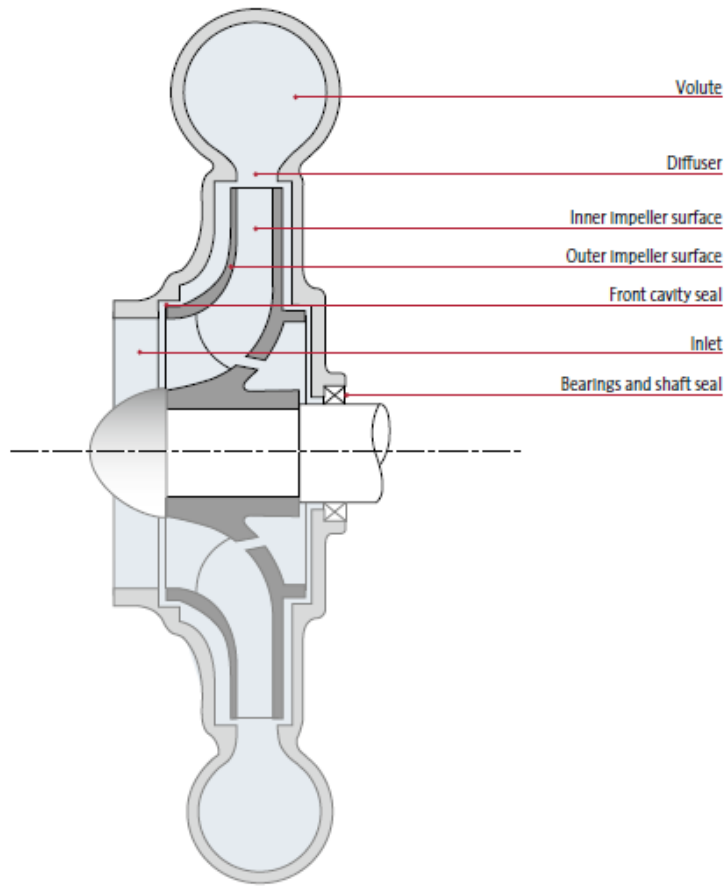


Figure 11: Loss causing components.[2]

### 3.1. MECHANICAL LOSSES

The mechanical loss differ from the pump type and consists of bearings, shaft seal and gear losses.

Bearing and shaft seal losses is caused by friction and is often modelled as constant. The losses is added as an increase of power to the total power consumption and vary with the rotational speed and pressure.[2]

For smaller pumps below 5kW the mechanical losses can consume a considerable portion of the coupling power.[7]

### 3.2. FLOW FRICTION

Flow or skin friction losses is a result of shear stresses on the boundary layers on the rotating impeller and pump casting surface.

The skin friction is dependent on the Reynolds number, the roughness of the surface and

fluid velocity relative to the surface.[7]

Friction causes a lower pressure which reduces the head. When the fluid velocity is increased the loss grows quadratically as the friction loss is dependent on the dynamic head multiplied with a dimensionless loss coefficient as seen in Eq. (21).

$$H_{loss,friction} = \zeta H_{dyn,in} = \zeta \frac{V^2}{2g} \quad (21)$$

Flow friction is often calculated individually for each component e.g. the inlet and outlet sleeve which is not effected directly by the impeller and can therefore be seen as a constant loss coefficient, where as the impeller, volute and return channel is a variable loss coefficient.[2]

### 3.3. CONTRACTION AND EXPANSION

At the pump inlet the area is reduced and thereby a contraction occurs (Fig. 12a). At the geometry edges, eddies is created and the flow is separated from a streamline parallel to the surface to curved streamlines.

The consequence of the contraction is an acceleration of the flow before a deceleration to fill the cross section which is causing a mixing loss that results in a head loss. As the contraction is often at the impeller eye, a round off of the inlet edges would considerably reduce the loss.

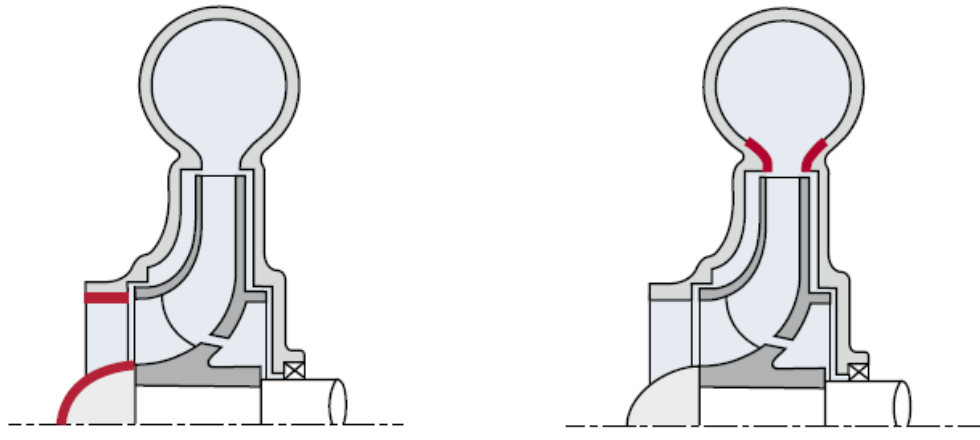


Figure 12

A mixing loss can also occur at the impeller outlet as an expansion (Fig. 12b) when the velocity energy is transformed to static pressure.

At sudden expansion water particles will no longer be moving with the same velocity which will cause internal friction in the fluid between the fluid particles.

Some of the velocity energy from after the cross section expansion is transformed into heat instead of static pressure and thereby a loss in head is obtained.[2]

### 3.4. RECIRCULATION LOSSES

When the pump is running at part load at a flow below the design point, recirculation zones in the hydraulic components can occur.

Recirculation zones seen on Fig. 13a reduces the effective cross section area as eddies with a velocity of zero is formed and constitute a considerable mixing loss.

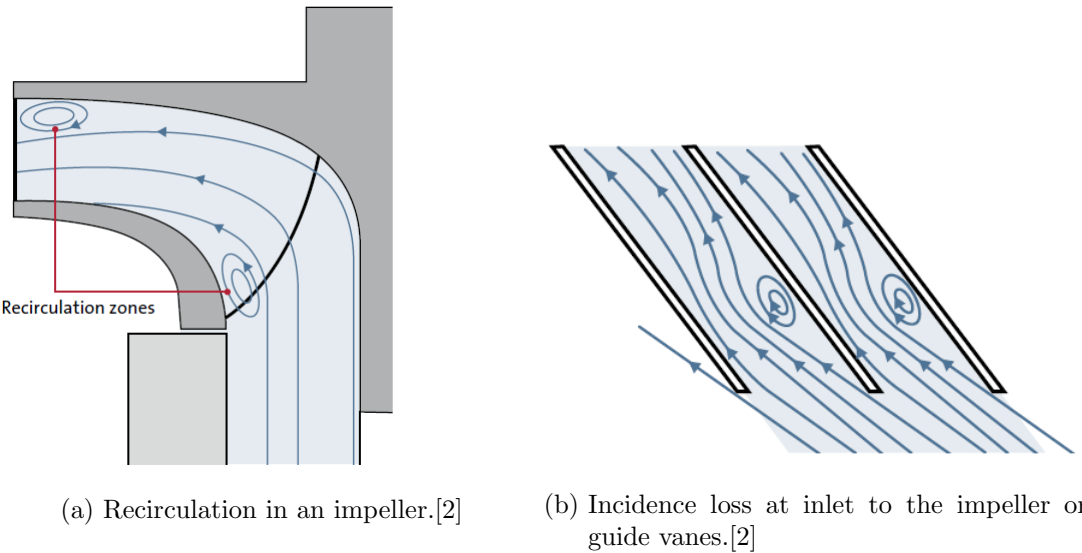


Figure 13

Recirculation zones does not occur at the nominal operating point and the pump performance can be predicted relatively precisely. At a partial load the head is reduced and/or the power consumption is increased which makes it difficult to estimate the pump curve. At part load an incidence loss is present when there is a difference between the blade and flow angle. Therefore to reduce incidence loss it is important to match blade angles and flow angles. To further decrease the incidence loss rounding of the blades leading edges is utilized. As the recirculation zone forms eddies and the flow is contracted, the flow must decelerate after the contraction to fill the vane and a mixing loss occur (Fig. 13b).[2]

### 3.5. DISK FRICTION

Disk friction occurs on the hub and the shroud of the impeller when it is rotating in the water filled pump casing.

As the impeller rotates the fluid between the impeller and the pump casing follows and creates a primary vortex. The fluid rotation velocity at the impeller surface equals the impeller velocity and is zero at the pump casing. The primary vortex average velocity is therefore assumed to be one half of the rotational velocity.

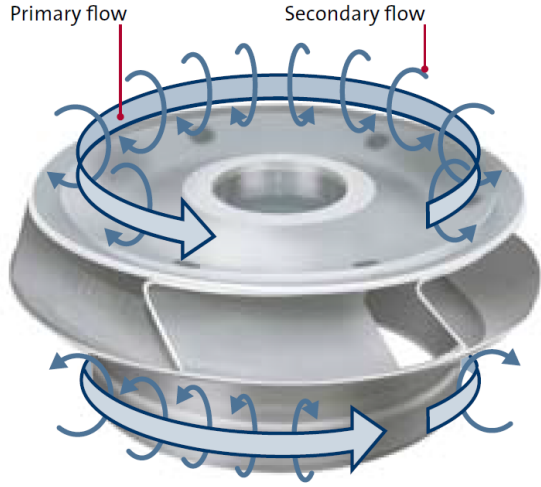


Figure 14: Primary and secondary vortex.[2]

A secondary vortex as seen on Fig. 14 is created by the centrifugal force because of difference in rotational fluid velocity between impeller and pump casing. This causes an increase of power consumption as the secondary vortex increases the disk friction by transferring energy from the impeller surface to the pump casing surface.

The disk friction is primarily dependent on the velocity but also distance between impeller surface and pump casing surface. The roughness of the impeller and pump housing also have an influence on the disk friction.[2]

### 3.6. LEAKAGE

Leakage occurs when fluid is circulating through small gaps. Different leakage losses is depended on the pump type but is always a loss between the rotating and fixed part of the pump.

For a radial pump without balancing holes the leakage often occur as a fluid circulating between the impeller eye and the pump casing as seen on Fig. 15.

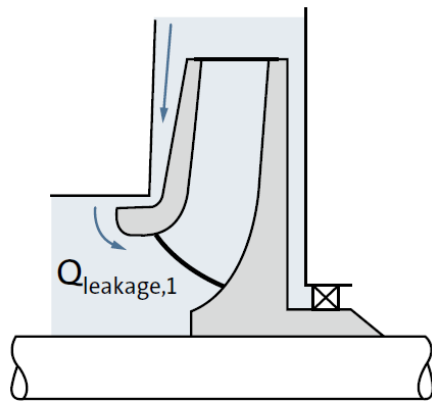


Figure 15: Leakage between impeller eye and pump casing.[2]

The impeller flow rate is equal to the flow from the leakage loss plus the normal flow rate as seen in Eq. (22).

$$Q_{impeller} = Q + Q_{leakage} \quad (22)$$

This result in a larger flow through the impeller compared to the flow through the entire pump and thereby a loss in efficiency.[2]

### 3.7. SUMMARY

These losses should be taken into consideration when designing an impeller. Individual mechanical and hydraulic types of losses which can occur in a pump is explained and how they affect the power consumption, head and flow. An incorporation of these losses will be considered in the impeller design models explained in Sec. 4.

## 4. IMPELLER DESIGN

The new impellers will be designed based on the existing Grundfos impeller. The design parameters and fixed dimensions for fitting the impeller in the pump housing is in Table 2.

Symbol	Definition	Value
$Q$	Flow rate	$28m^3/h$
$H$	Head	$23.4m$
$n$	Rotational speed	$2900rpm$
$d_s$ & $d_1$	Impeller inlet diameter	$0.064m$
$d_n$	Hub diameter	$0.032m$

Table 2: Fixed parameters.

Two different calculation models from respectively Willi Bohl and his book "*Strömungsmaschinen 2*" and Johann Friedrich Gülich with "*Centrifugal pumps*" are used for the design purpose. An impeller will be designed for each calculation model and compared to the pump performance curve of the existing impeller.

As the two models is using different symbols for the same notation, it is chosen to use their individual notation throughout the explanations and calculations. The calculations for Bohl can be found in App. B and for Gülich in App. C.

#### 4.1. WILLI BOHL CALCULATION MODEL

A sketch of the impeller with the different dimensional values is illustrated in Fig. 16.

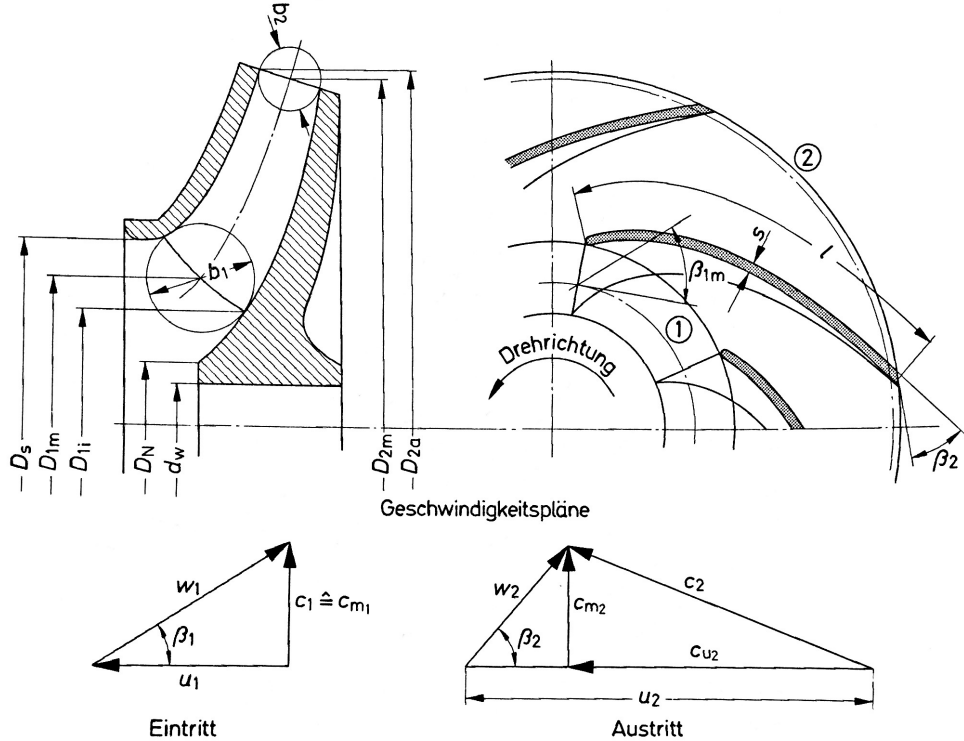


Figure 16: Impeller sketch from Strömungsmaschinen 2.[5]

The impeller outlet is chosen as vertical, meaning  $D_{2m} = D_{2a}$ .

##### 4.1.1. IMPELLER OUTER DIAMETER

At first the specific speed is calculated, which characterizing the type of pump. This is found with Eq. (23)

$$n_q = n \frac{\sqrt{Q}}{H^{3/4}} \quad (23)$$

Where  $n$  is the rotational speed,  $Q$  is the flow rate and  $H$  is the head. The specific speed is a comparative tool and the unit is seen as meaningless. It has no basis for further mathematical operations and relates to the physical geometry of the impeller. The specific speed unit is therefore considered dimensionless. The head coefficient which is a dimensionless parameter, is to be determined to calculate the impeller outer diameter by Eq. (24).

$$\Psi = \frac{2}{n_q^{2/3}} \quad (24)$$

This equation is only valid for a specific speed between  $15 \leq n_q \leq 60$ .  
The specific work done by the impeller blades can be calculated by Eq. (25).

$$Y = gH \quad (25)$$

Then the outer diameter of the impeller can be determined by Eq. (26).

$$D_{2a} = 0.45 \frac{1}{n} \sqrt{\frac{Y}{\Psi}} \quad (26)$$

#### 4.1.2. BLADE INLET HEIGHT AND OUTLET ANGLE

The blade height  $b_1$  and  $b_2$  as seen on Fig. 16 is determined based on the coefficients  $k_{m1}$  and  $k_{m2}$  which has to be read of the graph seen on Fig. 17.

Also the blade outlet angle,  $\tan(\beta_2)$ , is read from Fig. 17.

To minimize errors with graph readings, the software "ScanIt" is used to make a fit of the curves.

The fits from  $k_{m1}$  and  $k_{m2}$  is as in Eq. (27) and (28).

$$k_{m1} = 0.0021n_q + 0.0963 \quad (27)$$

$$k_{m2} = 0.002n_q + 0.0586 \quad (28)$$

As the blade outlet angle is between two curves, the value is taken as an average between the curves,  $\tan(\beta_{2,avg})$ .

The curves is as in Eq. (29) and (30).

$$\tan(\beta_{2,upper}) = -3E - 07n_q^3 + 8E - 05n_q^2 - 0.0077n_q + 0.5803 \quad (29)$$

$$\tan(\beta_{2,lower}) = -2E - 07n_q^3 + 7E - 05n_q^2 - 0.0073n_q + 0.5414 \quad (30)$$

The blade outlet angle is determined by Eq. (31)

$$\beta_2 = \beta_{2,avg} \quad (31)$$

Bohl proposes based on literature a blade outlet angle of  $15^\circ$  to  $45^\circ$ , whereas a range of  $20^\circ$  to  $30^\circ$  is particularly recommended. The calculated blade outlet angle is  $22.8^\circ$  which is within the recommended range.

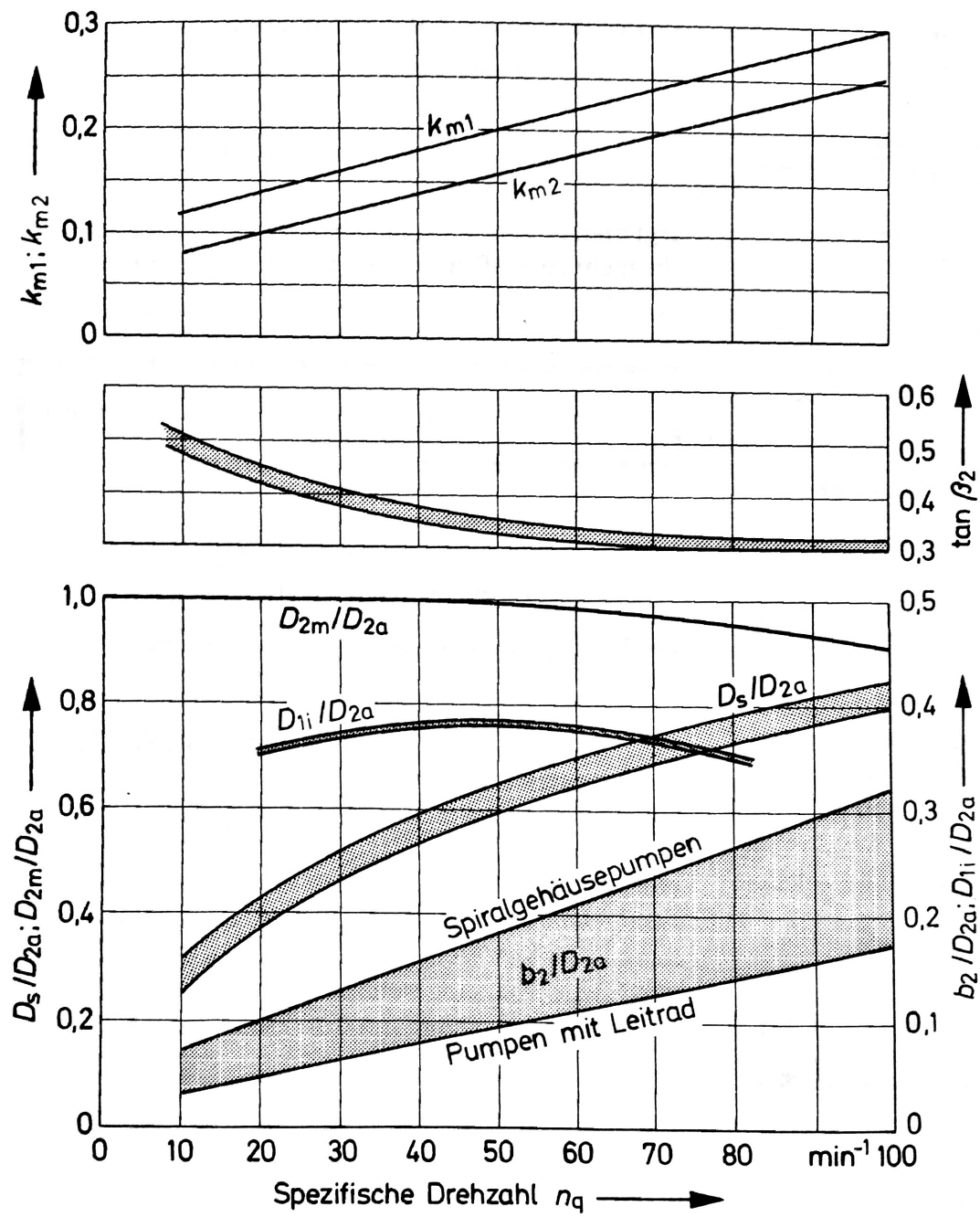


Figure 17: Determination of  $k_{m1}$ ,  $k_{m2}$  and  $\tan(\beta_2)$ .[5]

#### 4.1.3. BLADE INLET ANGLE

The blade inlet angle is dependent on the meridian velocity,  $c_{m1}$ , as seen on Fig. 16. The meridian velocity at the inlet and outlet is calculated by Eq. (32) and (33).

$$c_{m1} = k_{m1} \sqrt{2Y} \quad (32)$$

$$c_{m2} = k_{m2} \sqrt{2Y} \quad (33)$$

The blade inlet angle is found with Eq. (34).

$$\beta_1 = \tan^{-1} \left( \frac{c_{m1}}{u_1} \right) \quad (34)$$

Eq. (34) is dependent on the tangential velocity,  $u_1$ , which is determined in Eq. (35).

$$u_1 = D_{1m} \pi n \quad (35)$$

Here  $D_{1m}$  is defined as in Eq. 36.

$$D_{1m} = \frac{D_s + D_{1i}}{2} \quad (36)$$

Where  $D_{1i}$  is found with Eq. (37) with ScanIt from Fig. 17.

$$D_{1i} = (9E - 08n_q^3 - 5E - 05n_q^2 + 0.004n_q + 0.2867)D_{2a} \quad (37)$$

The recommended blade inlet angle is in the range of  $10^\circ$  to  $30^\circ$ . The calculated angle is  $20.19^\circ$ .

#### 4.1.4. NUMBER OF BLADES

When calculating the number of blades of the impeller, Bohl proposes a list of different empirically obtained equations. But as he recommends a blade number between 4-7 blades, only two of these formulas satisfy this condition.

For an estimation of the blade number, Bohl proposes Eq. (38) from relevant literature.

$$z \approx 2\pi \frac{D_{1m} + D_{2m}}{D_{2m} - D_{1m}} \sin \left( \frac{\beta_1 + \beta_2}{2} \right) \quad (38)$$

Another equation that satisfies the blade guide proposition of 5-7 blades is proposed by Prof. ECK and is as follows:

$$z \approx 8.5 \frac{\sin(\beta_2)}{1 - \frac{D_1}{D_2}} \quad (39)$$

Here  $D_1$  is identical to  $D_s$  and  $D_2$  to  $D_{2a}$ .

#### 4.1.5. BLADE OUTLET HEIGHT

The blade outlet height is dependent on the blade thickness coefficient  $k_2$  in Eq. (40).

$$k_2 = \frac{D_2\pi}{D_2\pi - z \frac{s_2}{\sin(\beta_2)}} \quad (40)$$

Here  $s_2$  is the blade thickness at the outlet. The blade thickness is chosen uniform for the entire blade,  $2.7mm$ .

The blade height can then be found with Eq. (41).

$$b_2 = \frac{Q}{D_{2m}\pi c_{m2}} k_2 \quad (41)$$

Where  $c_{m2}$  is found with Eq. (33). The necessary equations for the dimensions for construction of the impeller is found and the calculated values can be seen in the comparison section(Sec. 4.3). [5]

#### 4.2. JOHANN F. GÜLICH CALCULATION MODEL

A sketch of the impeller with the different length indications can be seen on Fig. 18.

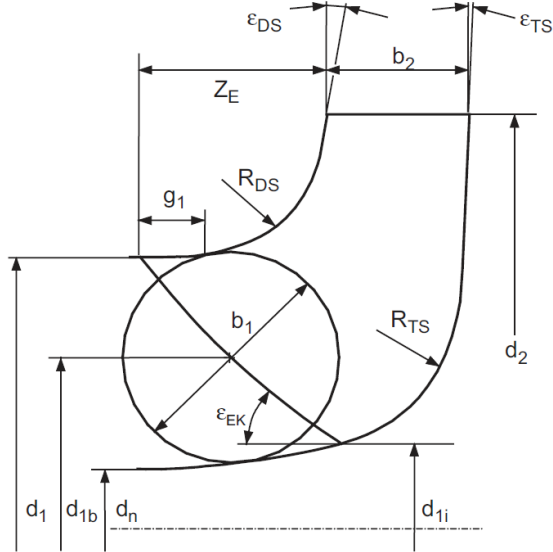


Figure 18: Impeller sketch.[7]

The extended velocity triangles of the impeller inlet and outlet is seen in Fig. 19

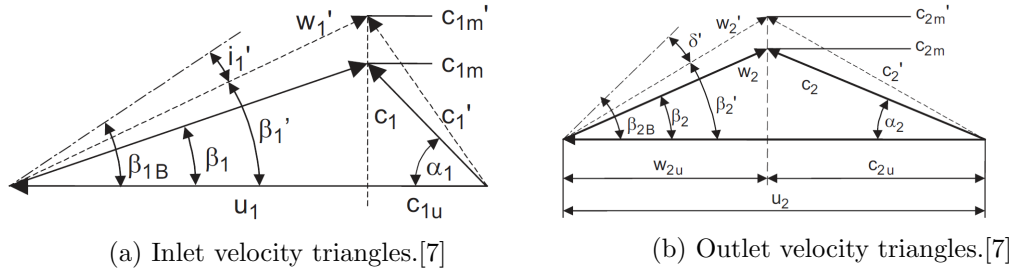


Figure 19

##### 4.2.1. IMPELLER OUTER DIAMETER

Again the specific speed is found with Eq. (23). The head coefficient can be chosen as a range between a lower and upper band as a function of the specific speed. A coefficient chosen in the lower band leads to a steeper Q-H curve with low risk of Q-H curve instability whereas a coefficient selected in the upper band a flatter Q-H curve and smaller impeller diameter is obtained but the risk of Q-H curve instability increases.

As Gülich has provided a formula for the head coefficient for the best efficiency point, this formula, Eq. (42), is chosen.

$$\Psi_{opt} = 1.21 \exp \left( \frac{-0.77n_q}{n_{q,Ref}} \right) \quad (42)$$

$n_{q,Ref}$  is the reference specific speed which is equal to 100.

The impeller outer diameter can then be found with Eq. (43).

$$d_2 = \frac{84.6}{n} \sqrt{\frac{H_{opt}}{\Psi_{opt}}} \quad (43)$$

#### 4.2.2. NUMBER OF BLADES AND OUTLET BLADE ANGLE

When selecting the number of impeller blades,  $z_{La}$ , it is proven that less than 5 blades can cause non-uniform flow over the circumference due to the blade spacing. 5 to 7 blades is recommended for a range of  $10 < n_q < 120$ .

The outlet blade angle can be calculated respectively to the slip factor, head and blade blockage with trial and error.

The blade blockage is the blockage effect the fluid experience when it enters or leaves the cascade due to the finite blade thickness. As the flow velocity have sudden changes in the meridional section it is possible to determine velocities with and without blockage. The following calculations will take blade blockage into account. The deflection caused by the blades is called the slip factor. As the flow does not follow the blades exactly, the flow is not blade-congruent. If the slip factor is 1 then there is no slip or deflection of the flow and therefore it is blade-congruent. The slip factor is primarily caused by the Coriolis force and the smaller it becomes the greater the deviation between the flow and blade angle is.

The slip factor can be calculated by Eq. (44).

$$\gamma = f_1 \left( 1 - \frac{\sqrt{\sin(\beta_{2B})}}{z_{La}} \right) k_w \quad (44)$$

Here  $f_1 = 0.98$  for a radial impeller and the  $k_w$  factor can be found with Eq. (45).

$$k_w = 1 - \frac{d_{1m}^* - \epsilon_{Lim}}{1 - \epsilon_{Lim}} \quad (45)$$

The  $\epsilon_{Lim}$  factor is determined with Eq. (46).

$$\epsilon_{Lim} = \exp \left( -\frac{8.16 \sin(\beta_{2B})}{z_{La}} \right) \quad (46)$$

The suction area can be found with Eq. (47).

$$A_1 = \frac{\pi}{4} d_1^2 - d_n^2 = \pi d_{1b} b_1 \quad (47)$$

The arithmetic average diameter at the impeller,  $d_{1b}$ , can be isolated in Eq. (47), and  $d_{1i}$  as seen in Fig. 18 can be calculated with Eq. (48).

$$d_{1i} = \frac{d_{1b}}{0.5 - d_1} \quad (48)$$

The geometric average diameter for the impeller can then be found with Eq. (49).

$$d_{1m} = \sqrt{0.5(d_{1a}^2 + d_{1i}^2)} \quad (49)$$

As it is the dimensionless quantity  $d_{1m}^*$  utilized in Eq. (45), Eq. (50) is applied.

$$d_{1m}^* = \frac{\sqrt{0.5(d_{1a}^2 + d_{1i}^2)}}{d_2} \quad (50)$$

The blade blockage is calculated with Eq. (51).

$$\tau_2 = \left( 1 - \frac{ez_{La}}{\pi d_2 \sin(\beta_{2B}) \sin(\lambda_{La})} \right)^{-1} \quad (51)$$

Here  $e$  is the blade thickness. The ratio between the blade thickness and impeller outer diameter should be in the range of 0.016 and 0.022. The ratio is chosen as 0.019.

$\lambda_{La}$  is the influence of blade inclination on blade blockage, which is the blade angle to the impeller shroud. This angle is chosen as  $90^\circ$  as the inlet blade angle between the hub and blade is often perpendicular, thus  $\alpha_1 = \lambda_{La}$  as seen on Fig. 19a

The head is calculated with Eq. (52).

$$H = \frac{\eta_{hyd} u_2^2}{g} \left( \gamma - \frac{Q_{La}}{A_2 u_2 \tan(\beta_{2B})} \left( \tau_2 + \frac{A_2 d_{1m}^* \tan(\beta_{2B})}{A_1 \tan(\alpha_1)} \right) \right) \quad (52)$$

The circumferential or tangential velocity,  $u_2$ , from the velocity triangle in Fig. 19b is found with Eq. (53), the outer area,  $A_2$ , with Eq. (54) and the hydraulic efficiency,  $\eta_{hyd}$ , is found in Fig. 20.

$$u_2 = \pi d_2 n \quad (53)$$

$$A_2 = \pi d_2 b_2 \quad (54)$$

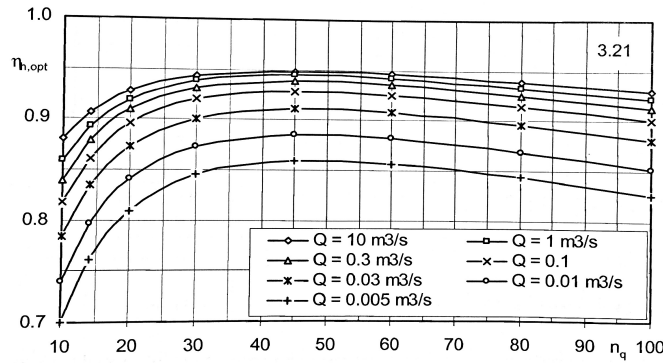


Figure 20: Optimum impeller efficiency.[7]

As Eq. (44), (46), (51) and (52) is all dependent on  $\beta_{2B}$  a numerical solver is needed. An initial guess for  $\beta_{2B}$  is needed and the error is calculated by the difference between the head calculated in Eq. (52) and the head chosen as the design point.

The number of blades was chosen to be 5 as the head only converged at this number of blades within the acceptable error of 0.03.

According to Gülich it is common for an impeller with 5-7 blades to have a blade outlet angle between  $15^\circ$  to  $45^\circ$ , but in most cases an angle of  $20^\circ$  to  $27^\circ$  is chosen. The calculated blade outlet angle is  $24.13^\circ$  which is within the recommended blade outlet angle range.

#### 4.2.3. BLADE OUTLET HEIGHT AND BLADE INLET ANGLE

Blade outlet height, blade outlet angle and blade number can not be determined individually as they are dependent on one another. Therefore the relative outlet height,  $b_2^*$ , is calculated based on empirical data. To obtain the best efficiency point with an uniform discharge flow,  $b_2^*$  is selected as small as possible to avoid turbulent dissipation losses. An empirical curve for the relative outlet height is presented by Gülich in Eq. (55).

$$b_2^* = 0.017 + 0.262 \frac{n_q}{n_{q,Ref}} - 0.08 \left( \frac{n_q}{n_{q,Ref}} \right)^2 + 0.0093 \left( \frac{n_q}{n_{q,Ref}} \right)^3 \quad (55)$$

The blade inlet angle,  $\beta_{1B}$ , is obtained by adding the incidence to the flow angle with blade blockage. The inlet blade blockage is determined with Eq. (56).

$$\tau_1 = \left( 1 - \frac{z_{La}e}{\pi d_1 \sin(\beta_{1B}) \sin(\lambda_{La})} \right)^{-1} \quad (56)$$

The blade inlet angle with blade blockage is calculated with Eq. (57).

$$\beta_1 = \tan^{-1} \left( \frac{c_{1m}\tau_1}{u_1 - c_{1u}} \right) \quad (57)$$

The meridional component of the absolute velocity is the flow rate divided by the inlet area ( $c_{1m} = Q_{La}/A_1$ )

The inner circumferential velocity,  $u_1$ , is calculated as in Eq. (53) with the inner diameter  $d_1$  instead of  $d_2$ .

The incidence which is the blade angle minus the flow angle, should be selected between  $0^\circ$  to  $4^\circ$ . An incidence angle of  $2^\circ$  is chosen for the calculations, as the inlet blade angle is:

$$\beta_{1B} = \beta_1 + i_1 \quad (58)$$

As Eq. (56), (57) and (58) are 3 equations with 3 unknowns the fixed point iteration method is used where an error of  $10^{-6}$  is chosen.[7]

As all parameters is found in both calculation models, the calculated values will be compared in the next section.

### 4.3. IMPELLER COMPARISON

The two calculation models is both generally based on empirical formulas. These formulas are created based on experience with designs that decreases losses that could cause inefficiency as explained in Sec. 3.

”Strömungsmaschinen 2” shows how to calculate the different design parameters but is missing to explain why the formulas is illustrated as they are regarding e.g. the reduction of losses. ”Centrifugal pumps” has a step by step calculation model where the different design parameters is described and how the different values in the formulas changes the pump performance and which losses is decreased.

There was made an error when finding  $D_{1m}$  in the Bohl model as it was seen as an average between  $D_N$  and  $D_s$  which was not the case. This caused the tangential velocity  $u_1$  to be underestimated, as per Eq. 36, which caused the blade angle to be overestimated. The error was discovered after the impeller had been produced therefore the impeller has the inlet angle  $\beta_1 = 23.35^\circ$  instead of the correct angle  $\beta_1 = 20.19^\circ$ . It has to be mentioned that this error only had an effect on the inlet blade angle and had no effects on any of the other dimensions. Also a small error was discovered after the Gülich impeller was constructed. The constant in Eq. (43) was written as 84.7 instead of 84.6 but also the gravitational acceleration was written as  $9.81 m/s^2$  instead of  $9.82 m/s^2$ . These typing errors had a small impact on the outer diameter which decreased by  $0.2 mm$  but also the blade outlet angle which decreased from  $25.73^\circ$  to  $24.13^\circ$ . The overestimation of the blade angle results in a decrease of tangential velocity of the absolute velocity and therefore an increase in head (Eq. (20)).

As the Bohl model has no formulas of the blade thickness, the thickness calculated in the Gülich model is used for both models. The calculated values from the two models is illustrated in Table 3.

Symbol	Willi Bohl (5 blade)	Willi Bohl (6 blade)	Johann F. Gülich (5 blade)
$D_s$ and $d_1$	64mm	64mm	64mm
$D_{2a}$ and $d_2$	137.2mm	137.2mm	140.9mm
$b_1$	16mm	16mm	16mm
$b_2$	8.6mm	8.7mm	10.6mm
$\beta_1$ and $\beta_{1B}$	$20.19^\circ$	$20.19^\circ$	$23.68^\circ$
$\beta_2$ and $\beta_{2B}$	$22.8^\circ$	$22.8^\circ$	$24.13^\circ$
$z_{La}$	5 blades	6 blades	5 blades
$s$ and $e$	2.7m	2.7m	2.7m

Table 3: Calculation model comparison.

The differences between the Bohl model with 5 and 6 blades is only the meridional outlet height, therefore only the 5 blade model will be created since the Grundfos and Gülich model also have 5 blades. There are four different parameters where the Bohl and Gülich models differ. The outer diameter is slightly larger for the Gülich impeller compared to the Bohl impeller and close to the Grundfos impeller at  $142mm$ . This will cause  $U_2$  to be larger for the Gülich impeller than for the Bohl impeller (Eq. (10) for the outer triangle). Therefore the head and flow rate would be expected to be larger for the Gülich impeller than the Bohl impeller and closer to the Grundfos impeller (Eq. (15) and (20)). A larger meridional outlet height,  $b_2$ , should also increase the head. Therefore the Gülich impeller head is expected to be larger than the Bohl impeller and close to the Grundfos impeller that has a meridional outlet height of  $10mm$ . The blade inlet angle error in the Bohl impeller might cause some incidence losses as the tangential velocity in the inlet velocity triangle has been underestimated (Eq. (11)). With the error, the difference between the blade inlet angles of Bohl and Gülich is  $0.33^\circ$  which means that the blade inlet angle should be of minor influence on the difference of their flow characteristics. The blade outlet angle for the Gülich impeller is larger than that of the Bohl impeller which should cause the head of Gülich to be larger than that of Bohl. The reason it is expected that the lifting height is higher, is that ideally a larger blade outlet angle should create a higher head. Even though the angle between the two models is close, the Bohl and Gülich impeller might experience some troubles as the combination of the two blade angels could cause a non uniform flow development and thereby create slip losses. Therefore it can be concluded overall that the impeller designed with Gülich is closer dimensionally to the Grundfos impeller and that its head is expected to be higher than the impeller designed with Bohl.

## 5. IMPELLER CONSTRUCTION

As all the design parameters of the impellers have been calculated in accordance with Bohl and Gülich, the construction is initiated. The impellers will be drawn in Autodesk Inventor Professional 2016 so that all dimensions are realized in a 3D sketch that can be printed.

### 5.1. MERIDIONAL SECTION

The meridional section is the first thing that is constructed of the impeller. The meridional section is what defines the hub and shroud shape of the impeller. For construction of the meridional section several dimensions must be selected, because the impeller needs to fit inside the Grundfos NK32-125/142 pump. Therefore all of the dimensional values have had to be identical to the original impeller except for the meridional channel width  $b$ , the outer diameter  $d_2$  and the blade angles. Since all these dimensions have been held constant the inlet meridional width,  $b_1$ , had to be moved down a bit in the meridional section. All dimensional values are illustrated by the Inventor sketch in Fig. 21.

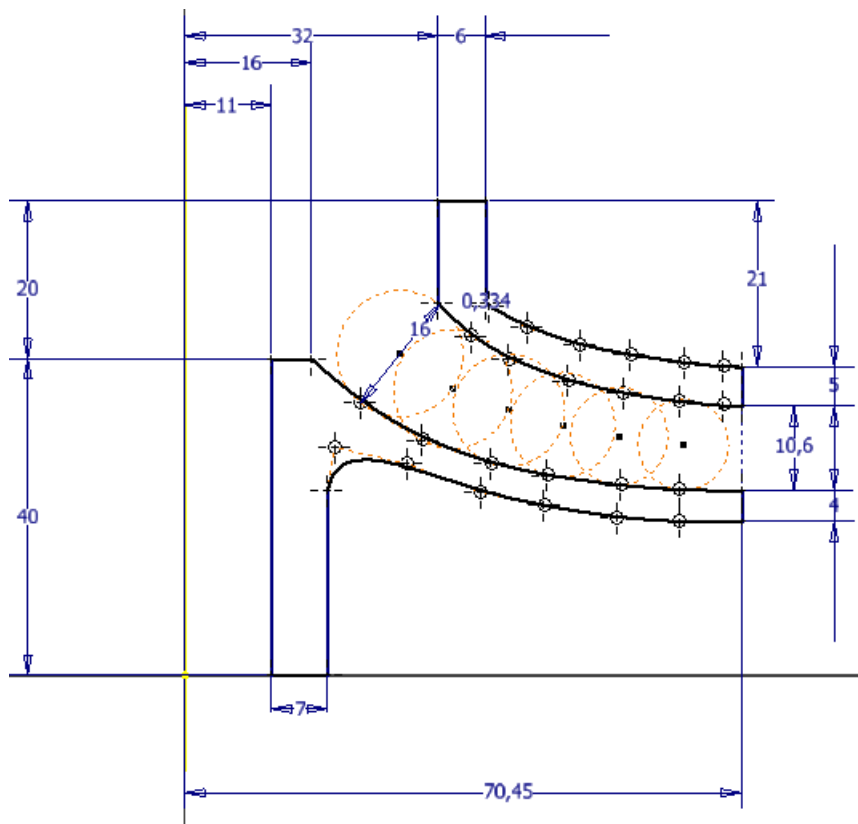


Figure 21: Sketch of the meridional section of the impeller according to the design parameters of Gülich. The meridional section sketch of the Bohl impeller is in App. E

The development of the meridional channel width has to be chosen so that the cross sectional area of the vane,  $A_k$ , vary continuously along the mean streamline. This means that the meridional section width has to develop along the length of the streamline and Gülich suggest doing this linearly between  $b_1$  and  $b_2$ . From Fig. 21 it can be seen that the linear development has not been followed all the way along the length of the mean streamline because this would have caused an upward curve of the inner streamline at the outlet of the impeller. Therefore the development of  $b$  is not entirely linear.

When the meridional section has been drawn it is rotated around the y axis and the finished hub and shroud shape is produced, and is illustrated in Fig. 22.

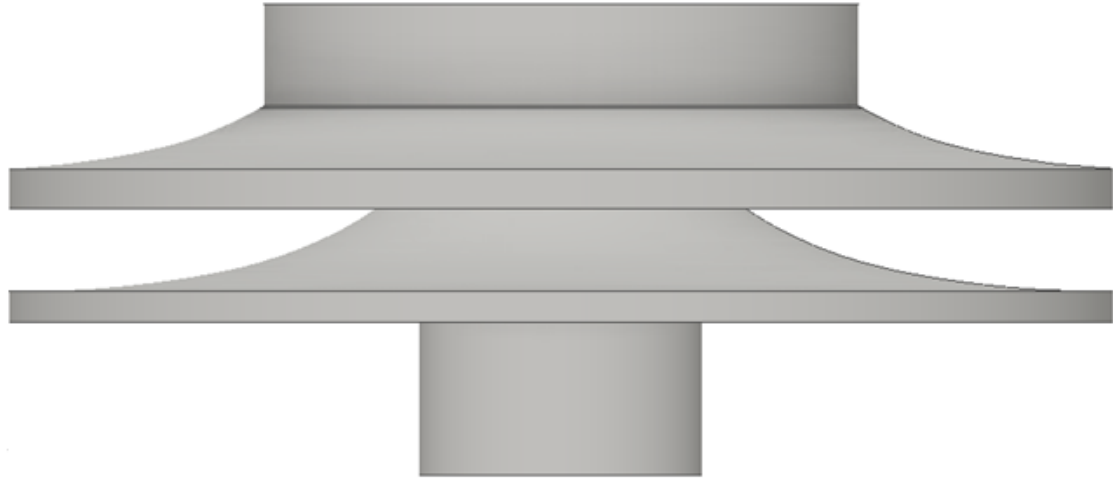


Figure 22: Side view of the impeller designed according to Gülich.

The last thing that needs to be done on the meridional is to make a cut so that it will fit on the pump shaft. The dimensions of this cut can be seen on Fig. 23 and the finished product on Fig. 24.

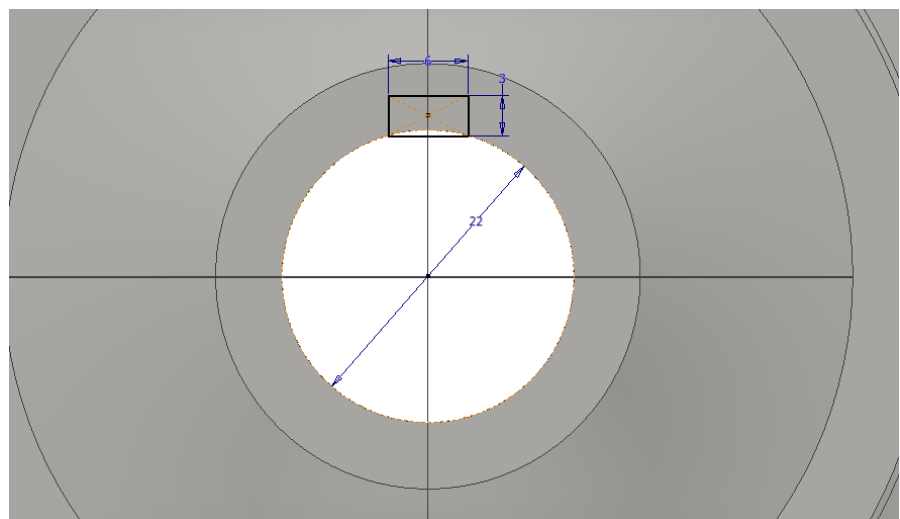


Figure 23: Cut made to fit impeller on the pump shaft.

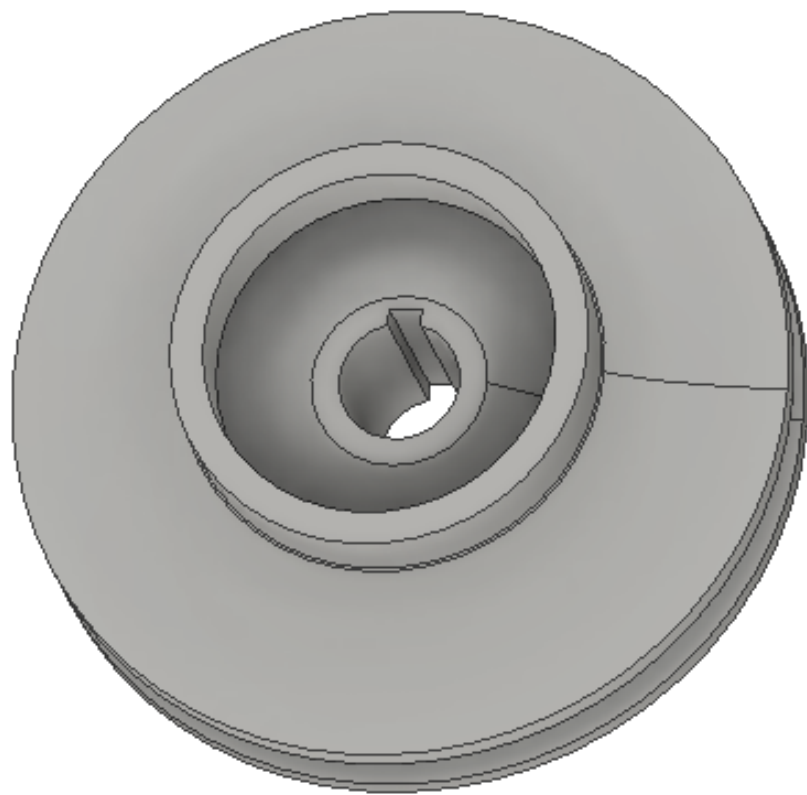


Figure 24: Finished 3D drawing of the impeller hub and shroud.

## 5.2. BLADE CONSTRUCTION

The blades will have to be drawn in such a manner that the blade inlet and outlet angles are maintained at the calculated values according to Sec. 4.1 and 4.2.

A method that will secure this, is the usage of circular arc blades. The method is suggested by both Bohl and GÜLICH, but GÜLICH has some reservations with the usage of this method that Bohl does not. According to GÜLICH, cylindrical blades are mainly used for radial impellers with a specific speed in the range of  $8 < n_q < 18$  for small pumps and for less demanding service up to a specific speed of around  $n_q = 25$ . Since the specific speed of all the impellers are  $n_q = 24.04$  it is assumed that the method will yield a sufficient result.

The circular arc blades are constructed through six stages[7] and a MATLAB script has been created to follow these and its output can be seen in Fig. 25.

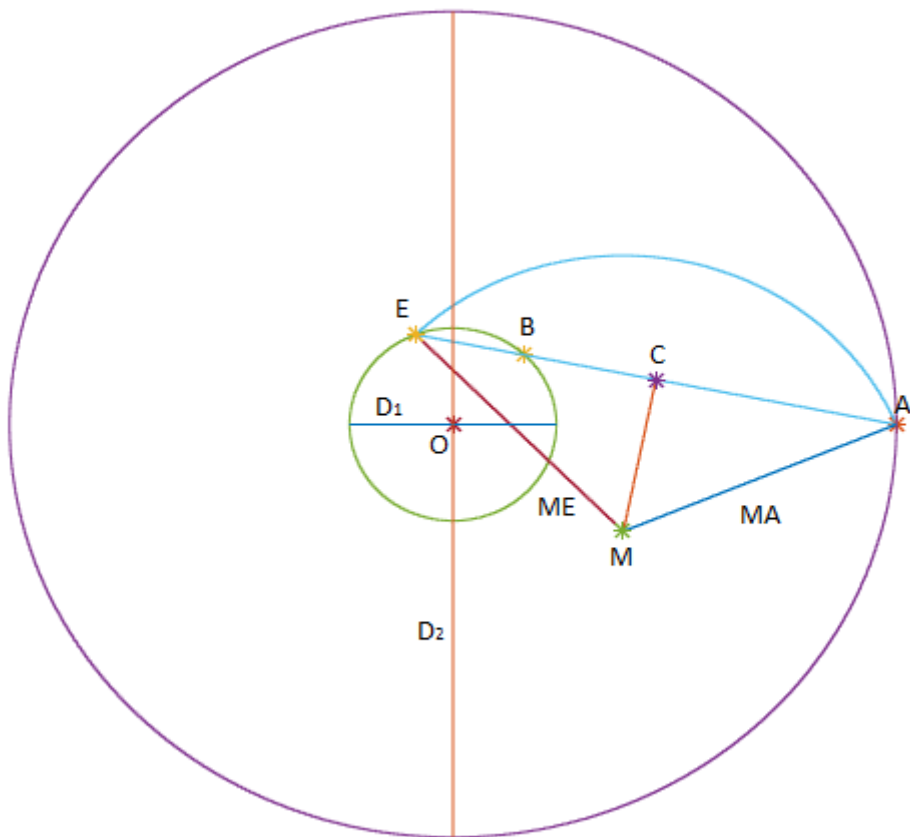


Figure 25: Circular arc blade coordinate in MATLAB.

The six steps are as follows:

1. Two circles with the diameters of the  $D_1$  and  $D_2$  are drawn with centroid at O.
2. The point A is defined on the outer circle. At point A the line MA is defined to be normal to the angle of  $\beta_2$ .
3. The point B is defined such that it intersects the inner circle at an angle of the sum of  $\beta_1$  and  $\beta_2$  from the line OA.
4. A line through point A and B intersects the inner circle at point E.
5. The normal at half the length of AE intersects the normal line MA at the point M, which is the center of the circular arc blade. The radius of this blade is:  $R_{sch} = |MA| = |ME|$ .
6. The arc created is the camber line of the blade and the pressure and suction surface is created with arcs having the radii's  $r = R_{sch} \pm 0.5 \cdot e$  around point M.

When the points A, E and M as well as the radius  $R_{sch}$  has been determined, the drawing process can begin. The sketch that can be drawn, is illustrated in Fig. 26.

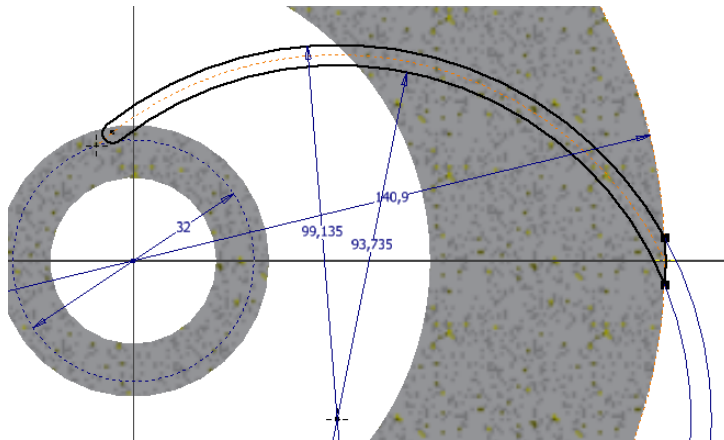


Figure 26: Inventor sketch of the impeller blade for Gülich. The sketch of the Bohl blade can be found in App. E

Then the blade leading and trailing edge profiles will have to be determined. The blade leading edge profile have been chosen to be a semi-circle with the diameter equal to the blade thickness, which for both impellers were 2.7mm. This is chosen despite Gülich not recommending it and only finding it acceptable for small pumps or applications with low requirements as the supplied pump. It has been chosen that there is not going to be a trailing blade edge profile. This means that the blade will be cut at the outer diameter  $d_2$  which means that the camber angle,  $\beta_2$ , is approximately the same as the pressure and suction side angles.[7] The semi-circular leading edge profile and the trailing edge are illustrated as they were drawn in Inventor in Fig. 26.

The last thing that had to be constructed was the development of the blades into the impeller eye. Since neither Bohl or Gülich touches upon this subject, it was decided to try to mimic the original Grundfos impeller. The reason neither Bohl or Gülich touches upon this, is that they use an 2D impeller design whereas Grundfos utilizes 3D impeller design coupled with Computational Fluid Dynamics. The original Grundfos impeller blade will curve and twist slightly as it reaches the impeller eye. The reason for this is that the impeller inlet angle can be varied over the leading edge profile to minimize the incidence loss and improve efficiency.[8]

The blade was constructed and the 3D sketch was finished as seen in Fig. 27. It can be seen on Fig. 27 that the blades have a smaller inlet profile which means that  $d_{1i}$ , illustrated in Fig. 18, is greater on both the Bohl and Gülich impellers compared to the Grundfos impeller. According to Gülich  $D_{1i}$  should be selected as small as possible for impellers with a specific speed less than approximately 25 to 30 to improve the stability of the head curve.[7]

There is also an edge at the top of the hub, that has been minimized, that might create recirculation zones in both the Gülich and Bohl impellers. These recirculation zones might reduce the head and the efficiency compared to the Grundfos impeller.

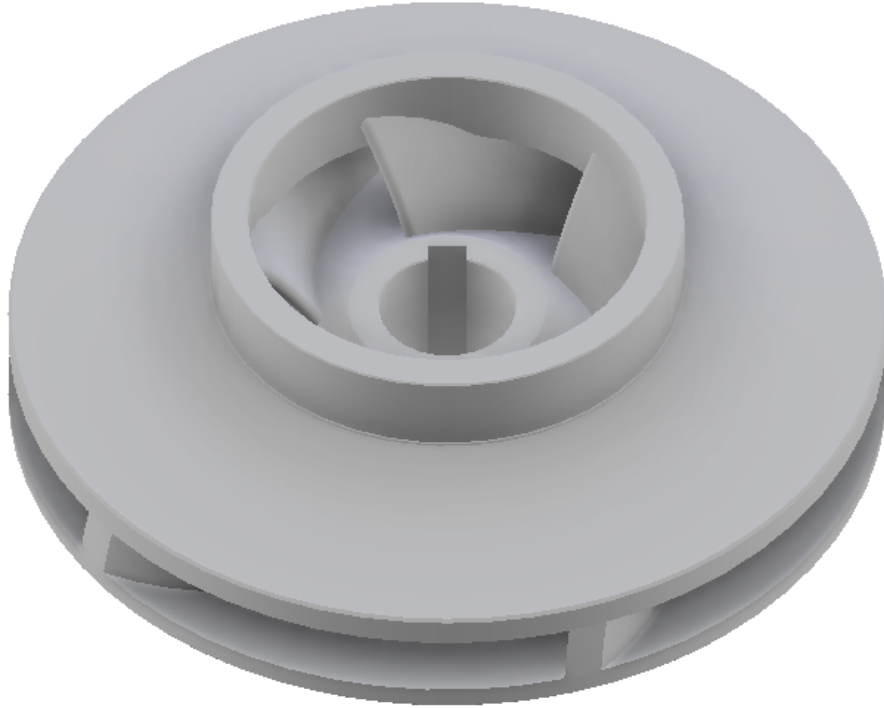


Figure 27: Inventor sketch of the impeller.

### 5.3. CROSS SECTIONAL VANE AREA

The cross sectional area of the vane is defined as in Eq. 59.[5]

$$A_k = a \cdot b \quad (59)$$

Where  $a$  is the channel width between the blades and  $b$  is the channel width in the meridional section. The development of  $a$  and  $b$  through the impeller is illustrated in Fig. 28.

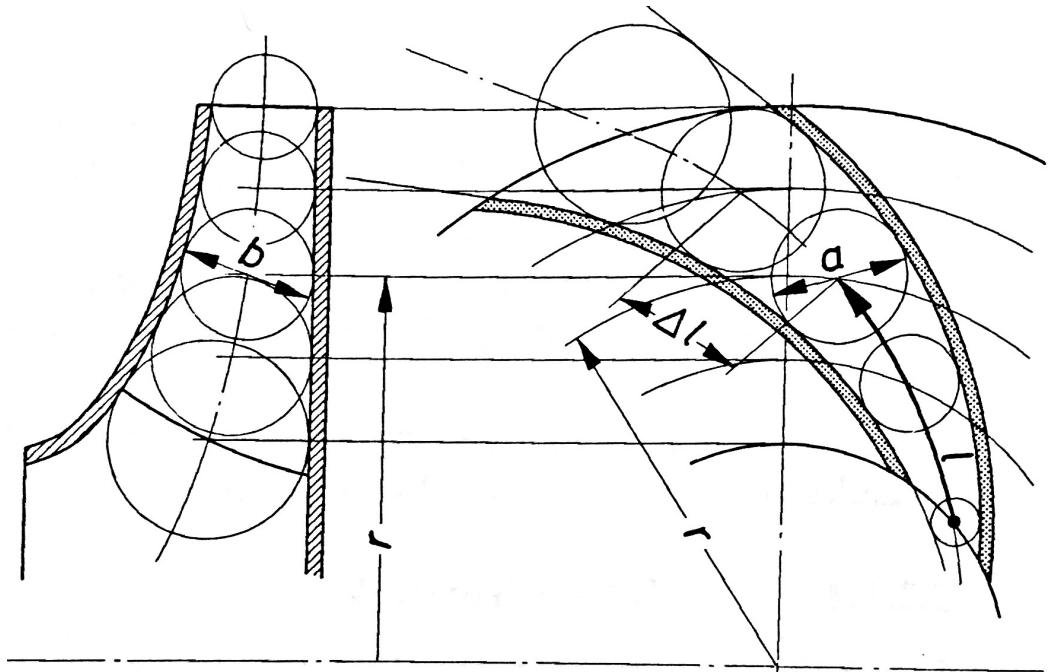


Figure 28: Illustration of  $a$  and  $b$ .[5]

According to both Bohl and Gülich the course of  $A_k$  must be continuous over the entire impeller.[5][7] This means that there should be no sudden changes or jumps of  $A_k$  along the vane. If this continues development is not achieved it could affect the flow negatively and cause mixing losses.

In Fig. 29 both the theoretical and actual vane area is illustrated for the impeller designed according to Gülich. The theoretical line was if the linear development of  $b$  was realized and the actual is made from measurements of the actual sketches made in Inventor. From Fig. 29 it can be concluded that if the linear development had been used, the vane area along the blade length would not have been continuous and there would have been sudden changes. The actual vane area development is more continuous and there is no jumps or sudden changes of values, since the vane area is constantly increasing. Only a minor change of the characteristic of the development of the vane area at the blade length around 49mm is influencing the curve tendency. Overall the actual vane area development seem to be better than if the linear development of  $b$  had been used strictly.

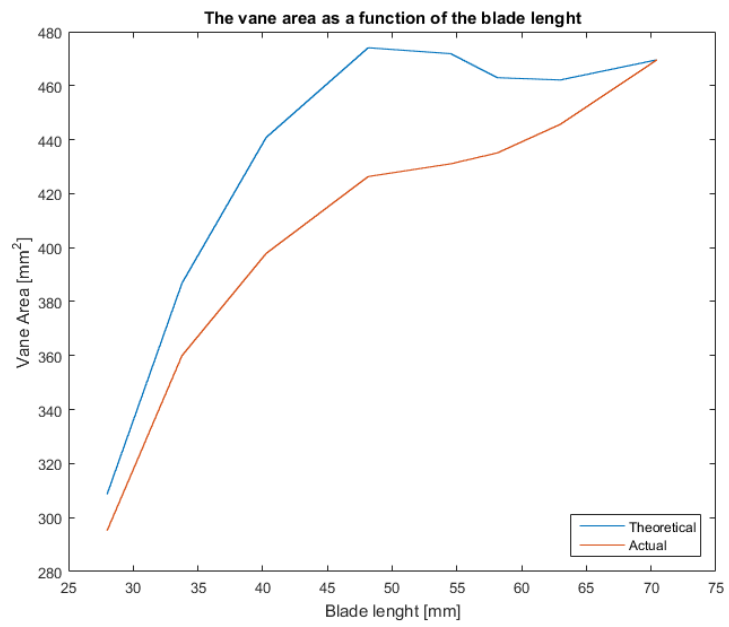


Figure 29: Illustration of the vane area's theoretical and actual development of the impeller designed with Gülich.

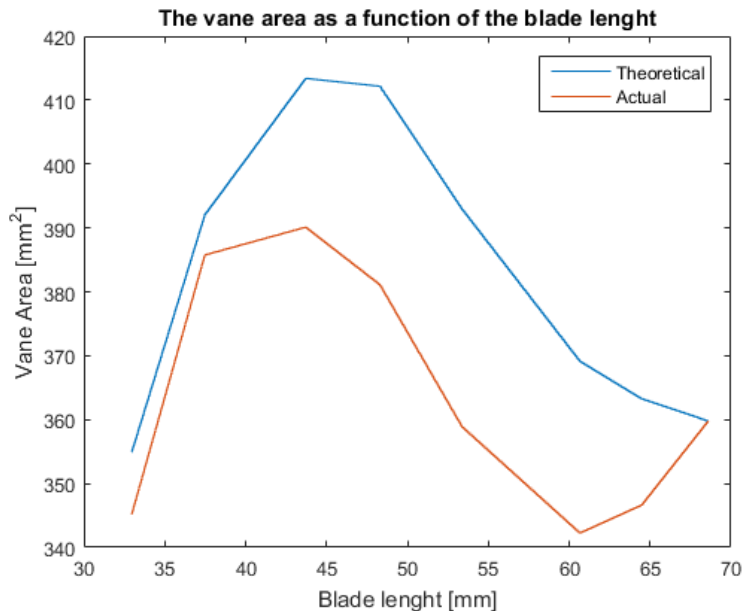


Figure 30: Illustration of the vane area's theoretical and actual development of the impeller designed with Bohl.

The development of the vane area of the impeller designed with Bohl is illustrated in Fig. 30. From this it can be seen that neither the theoretical linear development nor the actual development is consistent with how the vane area should. This means that the assumption that the development of  $b$  should be linear was a poor assumption in the case of the Bohl impeller. The increase and decrease of the vane area through the impeller will cause the water to accelerate and decelerate which will cause a mixing loss that could decrease the head compared to both the original Grundfos impeller and the impeller designed with Gülich.

Another of the arguments for not following the linear development is that  $\epsilon_{TS}$ , see Fig. 18, would not be zero which was one of the specifications in the calculations and common for radial impellers with  $n_q < 30$ [7].

## 6. TEST OF IMPELLERS

As explained in Sec. 2.1 the tests of the impellers was performed on the pump test stand at Aalborg University Esbjerg. To test the impellers, the pump had to be disassembled to mount the new impellers. At first the coupling shield was removed so that the coupling could be removed (Nr. 1 in Fig. 31). Then the pump house was unbolted from the stand (Nr. 2) before the pump house with the impeller could be untightened and pulled back (Nr. 3).

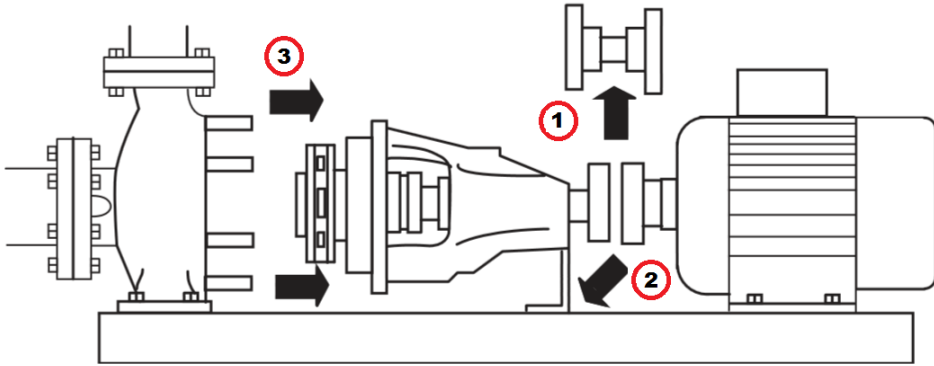


Figure 31: Change of impeller in the back pull pump.[1]

Then the impeller could be changed and the pump housing reattached and the impeller was ready for a performance test.

The pump was started by pressing the green button on the control station. As a pump performance program was already installed on the myRIO, this was started. Half an hour later the test was finished and the data was automatically transferred to a USB-key plugged into the myRIO. The pump was turned off by pressing the red button at the control station and the test was over.

The program was designed to measure the pressure, flow velocity, water tank temperature and power consumption. From these measurements the average flow rate, head, power consumption, efficiency and their respective standard deviations were calculated.

The standard deviation is calculated by Eq. (60) [9].

$$std = \sqrt{\frac{1}{n-1} \sum (x_i - \bar{x})^2} \quad (60)$$

$n$  is the number of readings and  $\bar{x}$  is the arithmetic mean of a repeated set of observations  $x_i (i = 1 \dots n)$ . The deviation can be used as an uncertainty of the measured values.

The new impellers were tested at the pump test stand two times for measurement similarity. In this section the experimental test of the impeller designs will be described and compared to the standard Grundfos impeller. The pump performance tests presented is from the first tests, the second tests can be found in App. F.

### 6.1. GRUNDFOS IMPELLER

According to the specifications on the pump the best efficiency point of the impeller should be a head of  $23.4m$  and a flow rate of  $28m^3/h$ .

The Grundfos impeller has the following known dimensions:

Symbol	Definition	Value
$d_2$	Impeller outlet diameter	$14.2cm$
$d_1$	Impeller inlet diameter	$6.4cm$
$d_n$	Hub diameter	$3.2cm$
$b_2$	Outlet blade height	$1.0cm$

Table 4: Grundfos impeller dimensions.

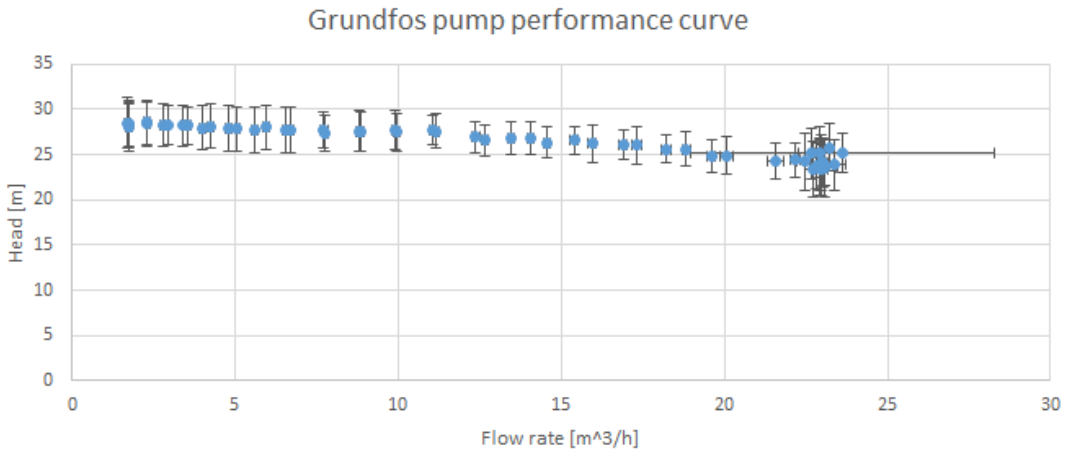


Figure 32: Performance curve of the Grundfos impeller.

The Grundfos impeller were tested in the pump test stand and its performance curve can be seen in Fig. 32. It can be seen that the best efficiency point is not reached as the flow rate never reaches the value of  $28m^3/h$ . The reason that the flow rate was limited to be below the design flow rate, must be because of the flow friction caused by the ball valves. Furthermore it was not possible to obtain the power usage of the pump since the power meter sends its maximum base value to the test setup. This meant that a constant power consumption was measured and the increasing development of the efficiency curve was obtained caused by the increase of the hydraulic power.

The pump performance curve from Grundfos's WebCAPS is seen in Fig. 33.

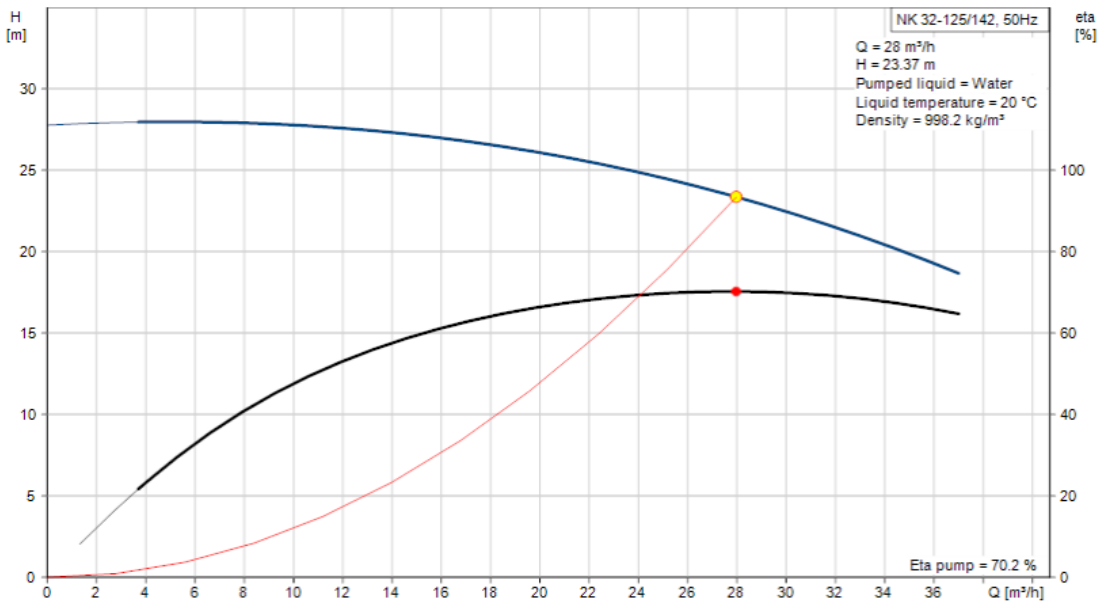


Figure 33: Performance curve for the Grundfos impeller from WebCAPS.[10]

The curve is measured by Grundfos. Comparing the curves in Fig. 32 and 33 they have the same tendency. The curve measured at AAUE has a faster drop in head compared to the curve from WebCAPS but as the standard deviation is approximately  $\pm 2 - 3m$  therefore the two curves are very similar. This meant that the operation head of  $23.4m$  was reached at  $22.7 - 23m^3/h$ .

## 6.2. WILLI BOHL IMPELLER DESIGN

The impeller designed with Bohl's design model was tested and the following pump performance curve, as seen on Fig. 34, was obtained.

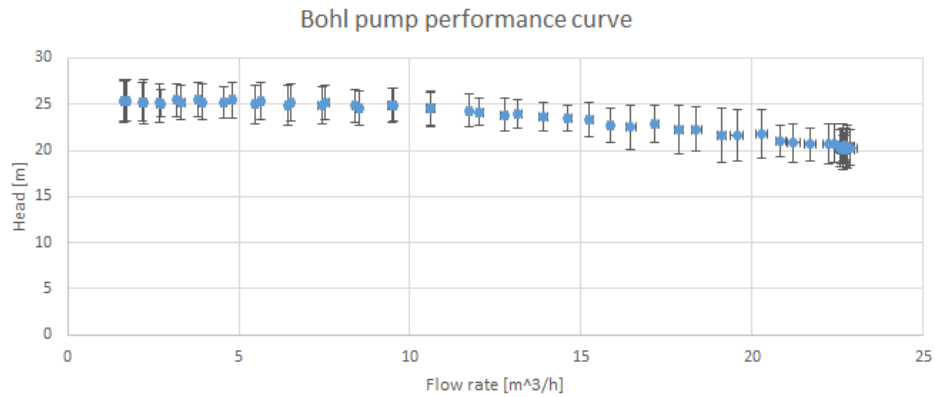


Figure 34: Test 1 of Bohl impeller.

The head has a tendency to drop as the flow rate increases as expected per Sec. 2.3. The pump performance curve never reaches the flow rate of the design specification at  $28m^3/h$ , but the head of  $23.4m$  was reached at a flow rate of  $15.3m^3/h$ . If the curve is compared to the standard Grundfos impeller (Fig. 35) the tendency follows that of the Grundfos impeller.

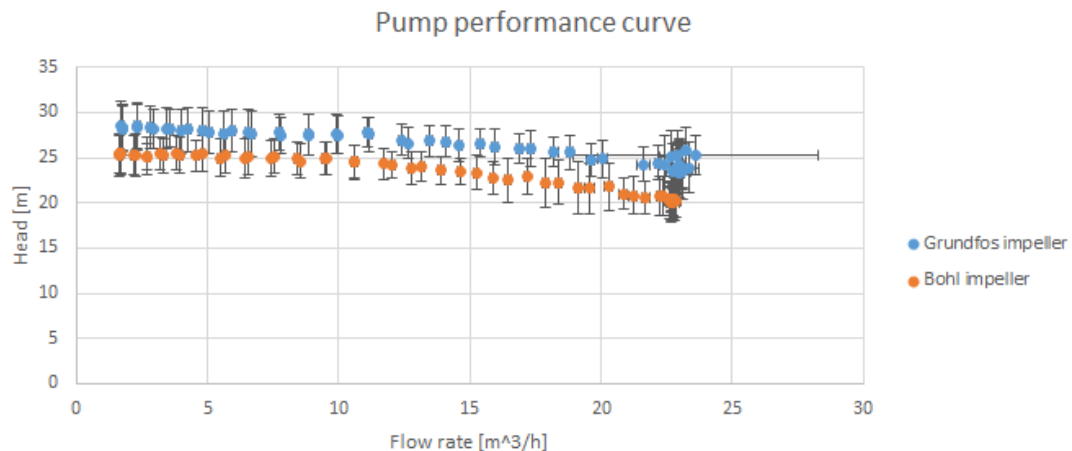


Figure 35: Bohl performance curve compared to Grundfos test performance curve.

As seen on Fig. 35 the impeller designed with Bohl has a constantly lower head curve compared to the original Grundfos impeller. If the standard deviation lines is examined, the Bohl curve is nearly within the deviation of the Grundfos curve.

Therefore it seems that the expectation of a lower head than the Grundfos impeller discussed in Sec. 4.3 was correct.

The reason for the curve deviation could be the smaller impeller diameter, which causes a decrease in the head and flow rate as described in Sec. 2.2.1 and discussed in Sec. 4.3. Also the blade inlet angle error of  $3^\circ$  could have an effect on the impeller performance. Normally the angle is added by an incidence of  $0^\circ - 4^\circ$  (Sec. 4.2.3) but as the inlet angle is based on empirical formulas, is expected that it have been taken into account. The vane area development discussed in Sec. 5.3 could also cause an unwanted flow development, i.e. mixing flow in the impeller which could cause a further decrease in head.

### 6.3. JOHANN GÜLICH IMPELLER DESIGN

The impeller design from Gülich have also been tested and the pump performance curve in Fig. 36 was obtained.

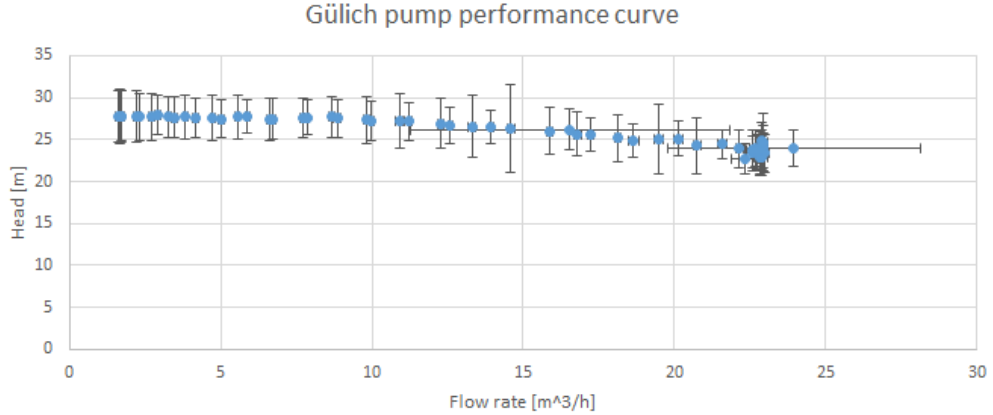


Figure 36: Test 1 of Gülich impeller.

As with the Bohl impeller, the flow never reaches the operation flow rate of  $28m^3/h$  but the head of  $23.4m$  is obtained at  $22.6 - 23m^3/h$ .

The curve is smooth until the flow rate is at its maximum, where small deviations caused by measurement errors is explored. Fig. 37 compare the Grundfos and the Gülich curve.

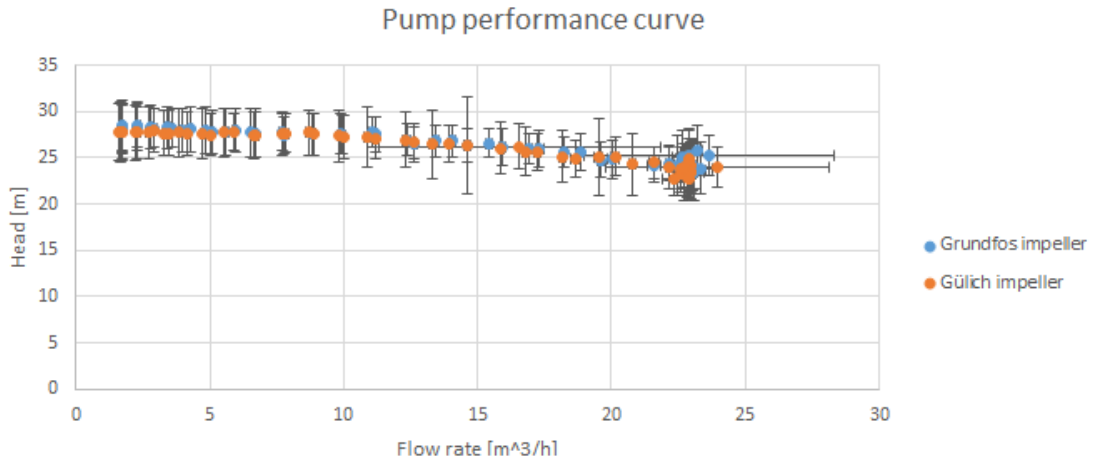


Figure 37: Gülich performance curve compared to Grundfos test performance curve.

The Gülich impeller curve follow the Grundfos curve with only a small deviation in head. Some of the points is even on top of each other, which is a very acceptable result. The small deviation in head is possibly the deviation in impeller outer diameter, as the Gülich model is  $1.1mm$  smaller than the Grundfos model.

#### 6.4. SUMMARY

Comparing the Grundfos, Bohl and GÜLICH impeller it is concluded that the Grundfos and GÜLICH impellers performance were very reminiscent of each other and Bohl had a performance curve with a constantly lower head than the two other impellers.

Therefore it would seem that the differences discussed in Sec. 4.3 did have the expected results. It was expected that the Bohl impeller would have a lower head than both the Grundfos and GÜLICH impellers, because of the smaller outer diameter, a smaller meridional section outlet height, losses caused by the error in the blade inlet angle and a smaller blade outlet angle.

Furthermore the problem with the development of the vane area in the Bohl impeller, discussed in Sec. 5.3, could also have caused a lower head because of mixing losses compared to the GÜLICH and Grundfos impellers.

The small error in the blade outlet angle of the GÜLICH impeller explained in Sec. 4.3 could cause slip losses as the blade inlet and outlet angle did possibly not follow the fluid angle. This error could possibly explain the small deviation between the Grundfos and GÜLICH curve together with the deviation in the outer diameter.

According to the experiments it can be concluded that the impeller developed with Bohl had underestimated several variables as the impeller designed with GÜLICH has several variables that are very close to the Grundfos impeller and has a performance curve that is very close to the Grundfos impeller.

## 7. DISCUSSION

It was determined that the key subject of this project was to design an impeller for a specific operation point. Therefore it was determined that the project would not contain any information of laws or ISO-standards for centrifugal pumps. The existing pump test stand had already been constructed in accordance with the ISO 9906 standard for pump tests to comply with its measurement requirements. Another thing that was not investigated was the volute of the pump housing. The reason was that there already was an existing pump housing in the test stand and an individual optimization of the volutes for the impellers would deviate from the project's focus point. Though the pump test stand was created in accordance with the ISO standard it did not work perfectly throughout the entire project period. At the start of the project period none of the experimental data were in accordance with the expected characteristics of the existing Grundfos impeller. Both the head and flow rate was about a third of the expected results and the power consumption was constant at around  $-4W$ . Troubleshooting of the pump test stand showed that both the flow meter and the pressure gages measured correctly, that neither pipes nor valves were clogged and that the electronic valves functioned as expected. Therefore the program installed on the myRIO was examined for calculations errors and it showed to be in accordance with the documentation of the construction of the setup. Then troubleshooting of the pump motor rotational speed was done and it was concluded that the speed of the motor complied with the motor specification. In a last ditch effort it was investigated whether the rotational direction of the motor was correct and it showed that the rotation was indeed in the wrong direction. Since the motor is a 3 phase AC motor two phases were shifted to reverse the direction of rotation. After this the flow and pressure measurements of the pump was in accordance with expected results, but the flow rate of the pump was still not able to reach its design flow rate of  $28m^3/h$  with neither of the designed impellers with Bohl, Gülich or the original Grundfos impeller. The reason for this must be because of the flow friction caused by the ball valves. When the pump's rotational direction had been corrected the power meter's output changed from the minimum to the maximum output signal which meant that a constant power consumption of around  $2970W$  was measured with some sudden drops. This meant that the power consumption measurements were not correct and therefore the efficiency of the pumps could not be found. After this further troubleshooting and programming of the power meter was discontinued because of time constraints.

The design guides for both Bohl and Gülich is constructed of empirical formulas and design experiences. Therefore it would be interesting to see if there were any difference in design rules and/or the results which their respective guides yielded. Both Bohl and Gülich utilizes empirical formulas and seem to be in agreement about in what ranges blade angles should be in. But there were some differences in the results between the two models. The impeller designed with Gülich was generally larger than the one designed with Bohl. The blade outlet height  $b_2$  was smaller for the Bohl calculation model compared to both the Gülich and Grundfos impeller which were very similar. This must mean that the method of determining the blade outlet angle, blade outlet height and number of blades simultaneously, as suggested by Gülich, gives better result than

Eq. 41 suggested by Bohl both when comparing the dimensions and pump curve to the Grundfos impeller. The blade angles obtained with Bohl was overall smaller than the blade angles obtained with Gülich. This again contributed to the expectation that the head produced by the impeller designed with Gülich should be larger than that of the impeller designed with Bohl. It has to be mentioned that both the Gülich and Bohl impellers were produced with minor blade angle errors which is unfortunate. Since the errors were not great and did not effect the other dimensions, it did not change the expectations, which was also proven experimentally. Therefore it was concluded that the impeller designed with Gülich should produce a larger head, and have a pump curve more reminiscent of the Grundfos impeller, than the impeller designed with Bohl.

The construction of the impellers were done by 3D printing. This meant that the impellers were drawn in 3D CAD software which in this case was Autodesk Inventor Professional 2016. The skills to draw an impeller in Inventor was developed sufficiently, but the drawing method of the blades did give some minor unwanted effects. Because of the way the blade was swept up in the impeller eye it was not possible for the blade to start exactly at  $D_n$  and the trailing edge did not coincide exactly with the hub's outer edge. Both of these errors were deemed small, especially the error in the trailing edge, compared to the uncertainty of trying to sweep the blades up into impeller eye.

The assumption that the development of the meridional section height should be linear was not a good assumption for the Bohl impeller, but was decent for the Gülich impeller. This means that when the difference between  $b_1$  and  $b_2$  is large and over a relatively short distance with circular blades, as was the case for Bohl compared to Gülich, another development must be chosen.

The structural strength of the 3D printed impellers were not investigated and stress test of the impellers where not conducted, but there were no physical signs of any wear on neither the blades nor the shroud. Therefore it seems that 3D printing could be a viable alternative to the production of prototypes with moulds which is an expensive and time consuming process. It could also be interesting to see if a 3D printed impeller could be a viable replacement not just as a prototype for testing but for an end product, especially in smaller pumps, but this would require extensive research in the structural strength of the impeller and of the different 3D printing technologies available which were out of the scope of this study.

As explained before it was not possible to measure the power consumption of the pump or reach the design flow rate. Therefore the three impellers were tested and held up against the Grundfos impeller. It was concluded from the tests that the impeller designed with Bohl was undersized as the operation lifting height of 23.4m was already reached at a flow rate of  $23m^3/h$ . The impeller designed with Gülich, as expected, had a higher lifting height than the impeller designed with Bohl and furthermore it showed to be close to the original Grundfos impeller but because of the flow limitations of the test stand it never reached the design flow rate of  $28m^3/h$ . Because of the flow limitations and lack of power consumption measurements, it was impossible to ascertain that the impellers had their best efficiency point at the design point. Therefore they were compared with the Grundfos impeller's performance curve and if the operation was close to this it was expected that they had the same best efficiency point.

If the project would have continued, the power meter would have been programmed so that the power consumption could be measured and an efficiency calculated.

Normally when a smaller head is wanted at the same flow rate, the impeller is recessed which changes the blade outlet angle and lower the efficiency.[4][7] If the efficiency could have been obtained a smaller operation point could have been constructed with the two calculation models and investigated if a higher efficiency could be obtained compared to a recessed impeller. Also a NPSH test to obtain a NPSH curve, for cavitation analysis, could be added to the program on the myRIO, as the valve for reducing the inlet pressure before the pump was already installed.

## 8. CONCLUSION

The components of centrifugal pump was investigated with primary focus on the impeller. This gave an understanding of how the pump is functioning and which components that have the largest influence. It was concluded that the impeller had the biggest influence on the performance of the pump. It was also decided that the impeller should be closed because the working fluid was clear water and that the blades should have a backward curved blade profile to improve the efficiency. The pump performance curve was explained to give background knowledge as the designed impellers had to be evaluated based on their performance curves.

The velocity triangles was investigated to give an understanding on how the fluid and blade velocities behave ideally through the impeller. Because of different mechanical and hydraulic losses in the impeller and volute, this ideal behavior is not attainable. Therefore the different losses' effect on head, flow rate and power consumption was investigated.

Two different calculation models by Willi Bohl and Johann GÜlich was used to design impellers for a specific operation point. The purpose was to compare the two models and evaluate which impeller that was most similar to the original impeller by a performance test. At first the two models was compared theoretically, where dimensionally the GÜlich impeller was most similar to the Grundfos impeller. After the impellers were produced their performance was tested on the pump test stand. The tests confirmed that the impeller designed with Bohl produced a smaller head and lower flow rate than both the Grundfos impeller and the GÜlich impeller. This meant that the impeller designed with GÜlich had a smaller deviation from the Grundfos impeller and therefore a more satisfying performance compared to the impeller designed with Bohl. It was not possible to obtain the best efficiency point of the impellers as the power meter was only sending its maximum base value to the myRIO.

## REFERENCES

- [1] Eduardo Bilbao Torrontegui and Johannes Veje. Pump testing stand. B.sc. report, Aalborg University Esbjerg, 2014.
- [2] Grundfos. *The Centrifugal Pump*. Grundfos Management A/S, 1st. edition, 2008.
- [3] Bjarke Hansen et. al. *Pumpe Ståbi*. Nyt Teknisk Forlag, 3rd. edition, 2007.
- [4] Bruce R. Munson et. al. *Fundamentals of Fluid Mechanics*. John Wiley Sons, Inc., 7rd. edition, 2013.
- [5] Willi Bohl. *Strömungsmaschinen 2 - Berechnung und Konstruktion*. Vogel, 5rd. edition, 1995.
- [6] Igor J. Karassik et. al. *Pump Handbook*. Mc Graw Hill, 4rd. edition, 2007.
- [7] Johann F. Gülich. *Centrifugal Pumps*. Springer, 3rd. edition, 2008.
- [8] D. Fred Marshall and Joseph A. Cotroneo. Maximizing compressor efficiency while maintaining reliability. *Turbomachinery symposium*, 18, 1989.
- [9] Dansk Standard. *DS/EN ISO 9906*. 2rd. edition, 2012.
- [10] Grundfos. Nk 32-125/142 y1-f-s-e-baqe - 96832956 pump cuve. <http://product-selection.grundfos.com/product-detail.?custid=GMA&productnumber=96832956&qcid=105481907>(online, cited 03.06.16).

## APPENDIX

### A. CURRICULUM

The following knowledge, skills and qualifications should be basis for the bachelor project in energy for the 5th semester with specialization within thermal processes.

Knowledge:

- Have knowledge about the structure of flow machines and other thermal flow system components used in thermal energy systems.
- Have knowledge of the thermal mechanical limitations, that occur because of the dynamic influence of these systems.
- Have knowledge about the environmental circumstances associated with these technologies.
- Be able to understand scientific methods and theories.

Skills:

- Be able to perform analyzes in connection with thermal flow systems and flow system components.
- To have gain experimental experience with flow machines and flow system components.
- Be able to analyze and evaluate results from simulations and experimental work of flow machines and flow system components.

Qualifications:

- To be able to handle complex and development oriented situations in study and work context within the energy technical field, with a special view to thermal processes.
- Have the ability to be a part of academic and cross-curricular cooperation with an professional approach within the energy technical field.
- Be able to identify own learning needs and structure one owns learning in different learning environments within the energy technical field.
- To attain the ability to translate academic knowledge and skills within thermal processes to a practical problem and to be able to solve this.

## B. WILLY BOHL MATLAB SCRIPT

```

1 %% Design model based on Willi Bohl's "Str mungsmaschinen 2"
2 %% Given Quantaties
3 n = 2900; % Rotational speed [rpm]
4 Q_opt = 28/3600; % Operation Flowrate [m^3/s]
5 H_opt = 23.4; % Operational Lifting Height [m]
6 g= 9.82; % Gravitational acceleration [m/s^2]
7
8 %% Impeller outer diameter
9 n_q = n*sqrt(Q_opt)/H_opt^0.75 % Specific speed [-]
10 psi= 2/(n_q^(1/5)); % Head coefficient [-]
11 Y= g*H_opt; % Specific work [m^2/s^2]
12 D_2a= 0.45*1/(n/60)*sqrt(Y/psi) % Outer diameter [m]
13
14 %% Suction diameter
15 D_n= 0.032; % Hub diameter [m]
16 D_s= 0.064; % Inlet diameter [m]
17
18
19 %% Meridian inlet and outlet velocity
20 if 0 < n_q < 100
21 k_m1= 0.0021 * n_q + 0.0963; % Curve from ScanIt [-]
22 k_m2= 0.002 * n_q + 0.0586; % Curve from ScanIt [-]
23 end
24 c_m2= k_m2 * sqrt(2*Y); % Outlet meridian velocity [m/s]
25 c_m1= k_m1 * sqrt(2*Y); % Inlet meridian velocity [m/s]
26
27 %% Blade angle beta_1 and beta_2 (bohl)
28 D_1i = (9E-08 * n_q^3 - 5E-05 * n_q^2 + 0.004 * n_q + 0.2867) ...
29     * D_2a %Curve from ScanIt times D_2a [m]
30 D_1m = (D_s + D_1i)/2; % Geometric average diameter [m]
31 u_1= D_1m * pi * n/60; % Inlet circumferential speed [m/s]
32 beta_1= atand(c_m1/u_1) % Blade inlet angle [degree]
33
34 if 0 < n_q < 100
35     beta_2upper = -3E-07 * n_q^3 + 8E-05 * n_q^2 ...
36         - 0.0077 * n_q + 0.5803; % Curve from ScanIt [-]
37     beta_2lower = -2E-07 * n_q^3 + 7E-05 * n_q^2 ...
38         - 0.0073 * n_q + 0.5414; % Curve from ScanIt [-]
39     beta_2_avg = (beta_2upper+beta_2lower)/2; % [-]
40     beta_2= atand(beta_2_avg) % Blade outlet angle [degree]
41 end
42 %% Different calculation methods for the number of blades z
43 D_2m= D_2a; % [m]
44 z= beta_2/3 % Number of blades (Bohl) [-]
45 z= 2*pi*(D_1m+D_2m)/(D_2m-D_1m) ...
46     * sind((beta_1+beta_2)/2) % Number of blades (Bohl) [-]
47 z= 7.85*D_2m/1*(1-D_1m/D_2m) ...
48     /(log(D_2m/D_s)) % Number of blades (Bohl) [-]
49 D_1=D_s;
50 D_2= D_2a;
51 z= 8.5*sind(beta_2)/(1-D_1/D_2) % Number of blades (Prof. Eck) [-]
52 z= 5 % Number of blades [-]

```

```

53
54 %% Blade inlet and outlet height
55 s_2= 0.0027; % Blade thickness [m]
56 k_2= D_2a*pi/(D_2a*pi ...
57 - z *(s_2/sind(beta_2))); % Blade outlet thickness coefficient
58 b_2= Q_opt/(D_2m * pi * c_m2)*k_2 % Blade outlet height [m]
59 b_1= 0.5*(D_1-D_n) % Blade inlet height [m]

```

### C. JOHANN GÜLICH MATLAB SCRIPT

```

1 %% Design model based on Johann Friedrich Glich's "Centrifugal pumps"
2 %% 1. Given Quantities
3 n = 2900; % Rotational speed [rpm]
4 Q_opt = 28/3600; % Operation Flowrate [m^3/s]
5 H_opt = 23.4; % Operational Lifting Height [m]
6 f_q = 1; % Single impeller eye [-]
7 g= 9.82; % Gravitational acceleration [m/s^2]
8 n_q = n*sqrt(Q_opt/f_q)/H_opt^0.75 % Specific speed [-]
9
10 %% 2. Efficiency
11 eta_h_opt = 0.82 % Read from graph [%]
12 %% Impeller outer diameter
13 n_qref = 100; % [-]
14 psi_opt = 1.21 * exp(-0.77*n_q/n_qref); % Head coefficient [-]
15 d_2 = 84.6/n*sqrt(H_opt/psi_opt) % Outlet diameter [m]
16
17 %% Velocity triangle at impeller inlet
18 d_1= 0.064 % Inlet diameter [m]
19 d_n= 0.032; % Hub diameter [m]
20 A_1= pi/4 * (d_1^2-d_n^2); % Inlet area [m^2]
21 c_1m= Q_opt/A_1; % Meridional component of the absolute velocity [m/s]
22 u_1= pi * d_1 * n/60; % Circumferential inlet speed [m/s]
23 alpha_1= 90;% Angle between relative and tangential velocity [degree]
24 c_1u= c_1m ...
25 /tand(alpha_1); % Circumferential component of absolute velocity [m/s]
26 b_1= 0.5 * (d_1 - d_n) % Blade inlet height [m]
27 z_La= 5 % Number of blades [-]
28 e= d_2*0.019; %Blade thickness chosen between 0.016 and 0.022 [m]
29 i_1= 2; % Incidence chosen between 0 and 4 degree [degree]
30 lampda_La= 90; % Angle between vanes and side disks [degree]
31 tau_1 = 20; % Initial value [-]
32 beta_1B = 20; % Initial value [degree]
33 beta_1p = 20; % Initial value [degree]
34 Error=1;
35 nIter=0;
36 while Error > 10^(-6) % Fixed point iteration
37     nIter = nIter + 1;
38     tau_1g = tau_1;
39     beta_1pg = beta_1p;
40     beta_1Bg = beta_1B;
41
42     tau_1= (1-(z_La*e)/(pi * d_1 * sind(beta_1Bg) ...
43     *sind(lampda_La)))^-1; % Blade inlet blockage factor [-]
44     beta_1p= atand(c_1m * tau_1g ...
45     / (u_1 - c_1u)); % Blade inlet angle without incidence [degree]
46     beta_1B= beta_1pg + i_1; % Blade inlet angle with incidence [degree]
47
48     Error = max([abs(tau_1 - tau_1g) abs(beta_1pg - beta_1p) ...
49     abs(beta_1Bg - beta_1B)]);
50
51 end
52 beta_1B % Flow inlet angle with blockage [degree]

```

```

53 %% Blade outlet height
54 u_2= pi * d_2 * n/60; % Circumferential outlet speed [m/s]
55 b_2dot= 0.017+0.262*(n_q/n_qref)-0.08*(n_q/n_qref)^2 ...
56 +0.0093*(n_q/n_qref)^3; % Dimensionless blade outlet height [-]
57 b_2= b_2dot*d_2 % Blade outlet height [m]
58
59 %% Blade outlet angle
60 f_1= 0.98; % For radial [-]
61 d_1b= A_1/(pi * b_1); % Arithmetic average diameter [m]
62 d_1i= d_1b/0.5-d_1; % [m]
63 d_1a= d_1; % [m]
64 d_dot1m= sqrt(0.5*(d_1a^2 + d_1i^2)) ...
65 /d_2; % Dimensionless geometric average diameter [m]
66 A_2 = pi*d_2*b_2; % Outlet area [m^2]
67
68 beta_2Bg = 20; % Initial value [degree]
69 Error=1;
70 nIter=0;
71 while Error > 0.03
72     nIter = nIter + 1;
73     beta_2B = beta_2Bg;
74     epsilon_lim = ...
75         exp(-8.16*sind(beta_2B)/z_La); % Dimensionless parameter [-]
76     k_w = 1 -((d_dot1m-epsilon_lim) ...
77         /(1-epsilon_lim))^3; % Dimensionless parameter [-]
78     gamma = f_1 * (1- sqrt(sind(beta_2B))/z_La^0.7) ...
79         *k_w; % Slip factor [-]
80     tau_2 = (1-e*z_La/(pi * d_2 *sind(beta_2B) ...
81         * sind(lampda_La)))^-1; % Blade outlet blockage [-]
82     H = eta_h_opt*u_2^2/g *(gamma - Q_opt/(A_2 * u_2 * tand(beta_2B)) ...
83         *(tau_2 + A_2*d_dot1m*tand(beta_2B) ...
84             /(A_1*tand(alpha_1)))); % Head [m]
85
86     Error = abs(H_opt - H);
87     if Error > 0.03
88         beta_2Bg= beta_2Bg + 0.001;
89     end
90     if Error < 0.03
91         beta_2Bg = beta_2Bg - 0.001;
92     end
93 end
94 beta_2B % Flow outlet angle with blockage [degree]

```

## D. BLADE DESIGN MATLAB SCRIPT

```

1 %% Input values
2 D_1 = 3.2E1;
3 D_2 = 13.72E1;
4 r_1 = 0.5*D_1;
5 r_2 = 0.5*D_2;
6 beta_1 = 23.35;
7 beta_2 = 22.8;
8 beta_tot = beta_1 + beta_2;
9 z = 5;
10 s = 2.7;
11 %% Determine Angles for points A
12 A_ang(z) = 0;
13 for i = 1:z
14     A_ang(i) = (i-1)*360/z;
15 end
16 A_ang;
17 %% Determine Positions for points A
18 A(2,z) = 0;
19 for i = 1:z
20     for j = 1:2
21         if j == 1
22             A(j,i) = r_2 * cosd(A_ang(i));
23         else
24             A(j,i) = r_2 * sind(A_ang(i));
25         end
26     end
27 end
28 A;
29 %% Determine Angles for points B
30 for i = 1:z
31     beta_B(i) = beta_tot + (i - 1) * 360 / z;
32 end
33 %% Determine Positions for points B
34 B(2,z) = 0;
35 for i = 1:z
36     for j = 1:2
37         if j == 1
38             B(j,i) = r_1 * cosd(beta_B(i));
39         else
40             B(j,i) = r_1 * sind(beta_B(i));
41         end
42     end
43 end
44 B;
45 %% Determine Point E
46 OA = sqrt(A(1,1)^2 + A(2,1)^2);
47 BA = sqrt((A(1,1) - B(1,1))^2 + (A(2,1) - B(2,1))^2);
48 B1_ang = asind(OA * sind(beta_tot) / BA);
49 B2_ang = 180 - B1_ang;
50 O2_ang = 180 - 2*B2_ang;
51 %% Determine Angles for the points E
52 for i = 1:z

```

```

53     beta_E(i) = beta_tot + abs(O2_ang) + (i - 1) * 360 / z;
54 end
55 % Determine Positions for the points E
56 E(2,z) = 0;
57 for i = 1:z
58     for j = 1:2
59         if j == 1
60             E(j,i) = r_1 * cosd(beta_E(i));
61         else
62             E(j,i) = r_1 * sind(beta_E(i));
63         end
64     end
65 end
66 E;
67 %% Determine the points C
68 C = 0.5 * (A + E);
69 %% Determine the points M
70 AC = 0.5 * sqrt((A(1,1) - E(1,1))^2 + (A(2,1) - E(2,1))^2);
71 A_angout = 180 - B2_ang - beta_tot;
72 M_ang = 90 - A_angout - beta_2;
73 CM = sind(A_angout + beta_2) * AC / sind(M_ang);
74 M_0 = [CM * cosd(-A_angout - 90);
75         CM * sind(-A_angout - 90)];
76 M = M_0 + C(:,1);
77 % Determine Angles for the points E
78 for i = 1:z
79     beta_E(i) = beta_tot + abs(O2_ang) + (i - 1) * 360 / z;
80 end
81 % Determine Positions for the points E
82 E(2,z) = 0;
83 for i = 1:z
84     for j = 1:2
85         if j == 1
86             E(j,i) = r_1 * cosd(beta_E(i));
87         else
88             E(j,i) = r_1 * sind(beta_E(i));
89         end
90     end
91 end
92 %% Create blade points
93 R = sqrt((M(1,1) - A(1,1))^2 + (M(2,1) - A(2,1))^2);
94 for i = 1:2*M_ang
95     for j = 1:2
96         if j == 1
97             Blade_0(j,i) = R * cosd(i + 2*A_angout);
98             Blade(j,i) = Blade_0(j,i) + M(1,1);
99         else
100             Blade_0(j,i) = R * sind(i + 2*A_angout);
101             Blade(j,i) = Blade_0(j,i) + M(2,1);
102         end
103     end
104 end
105
106 A

```

```

107 E
108 M
109 D_plus = 2*(R + 0.5 * s)
110 D_minus = 2*(R - 0.5 * s)
111 %% Plot
112 % Generate outer circle of the impeller
113 for i = 1:1:361
114     for j = 1:2
115         if j == 1
116             out_c(j,i) = r_2 * cosd(i);
117         else
118             out_c(j,i) = r_2 * sind(i);
119         end
120     end
121 end
122 % Generate inner circle of the impeller
123 for i = 1:1:361
124     for j = 1:2
125         if j == 1
126             in_c(j,i) = r_1 * cosd(i);
127         else
128             in_c(j,i) = r_1 * sind(i);
129         end
130     end
131 end
132
133 % Point O
134 O = [0 0];
135
136 % Diameters
137 D_1 = [r_1 0;
138         -r_1 0];
139 D_2 = [0 r_2;
140         0 -r_2];
141
142 % Generate lines between points A and B
143 Lines_AE = [A(1,1) E(1,1); A(2,1) E(2,1)];
144 Lines_ME = [M(1,1) E(1,1); M(2,1) E(2,1)];
145 Lines_MA = [M(1,1) A(1,1); M(2,1) A(2,1)];
146 Lines_MC = [M(1,1) C(1,1); M(2,1) C(2,1)];
147
148 plot(A(1,1),A(2,1),'*',B(1,1),B(2,1),'*')
149 hold on
150 plot(out_c(1,:),out_c(2,:),in_c(1,:),in_c(2,:))
151 hold on
152 plot(Lines_AE(1,:),Lines_AE(2,:),Lines_ME(1,:),Lines_ME(2,:) ...
153 ,Lines_MA(1,:),Lines_MA(2,:),Lines_MC(1,:),Lines_MC(2,:))
154 hold on
155 plot(E(1,1),E(2,1),'*')
156 hold on
157 plot(C(1,1),C(2,1),'*')
158 hold on
159 plot(M(1,1),M(2,1),'*')
160 hold on

```

```
161 plot(Blade(1,:),Blade(2,:))  
162 hold on  
163 plot(O(1,1), O(1,2), '*')  
164 hold on  
165 plot(D_1(:,1),D_1(:,2))  
166 hold on  
167 plot(D_2(:,1),D_2(:,2))
```

## E. BOHL CONSTRUCTION SKETCHES

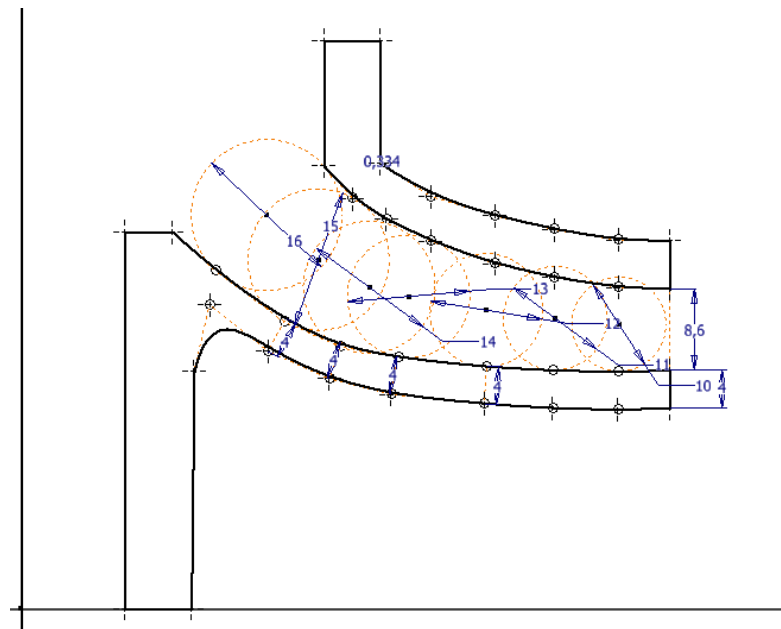


Figure E.1: Meridional sketch of the Bohl impeller.

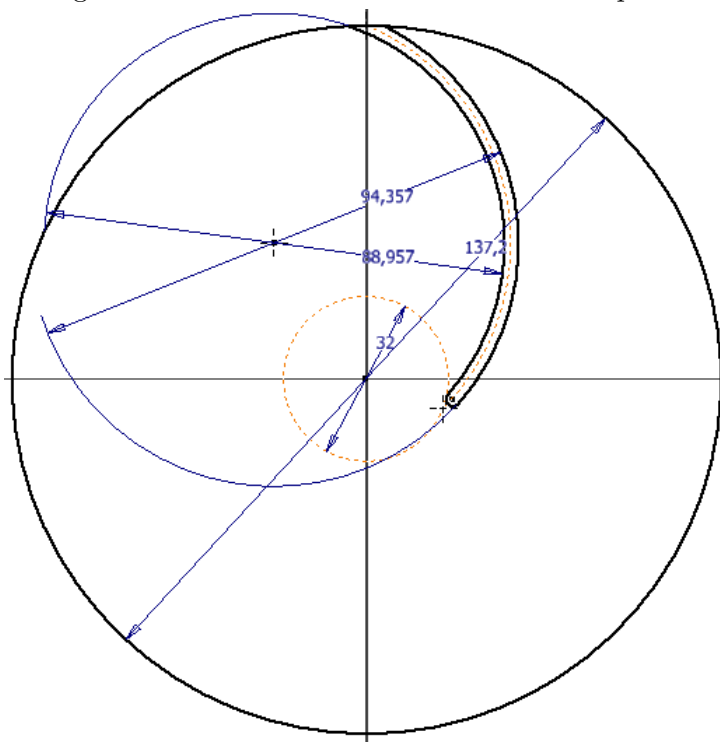


Figure E.2: Sketch of the blade of the Bohl impeller.

## F. IMPELLER TEST 2 GRAPHS

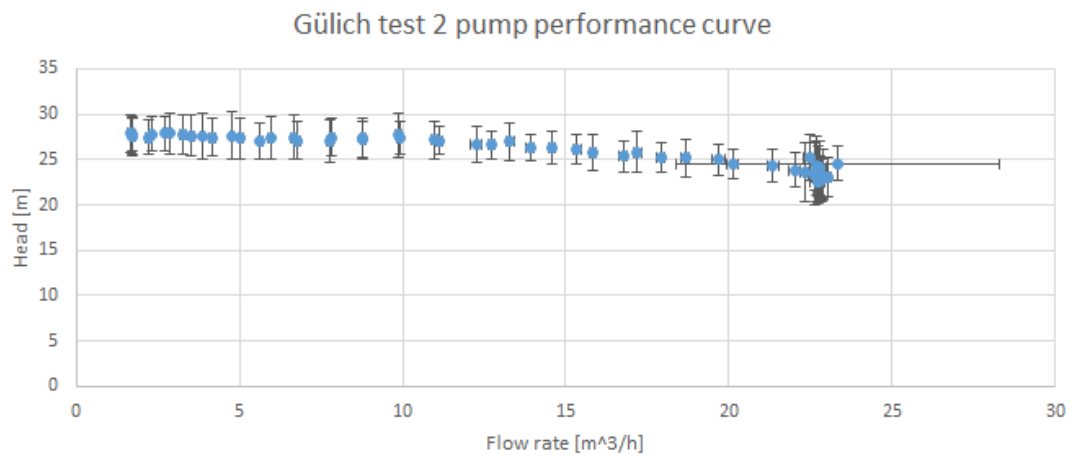


Figure F.1: Bohl impeller test 2

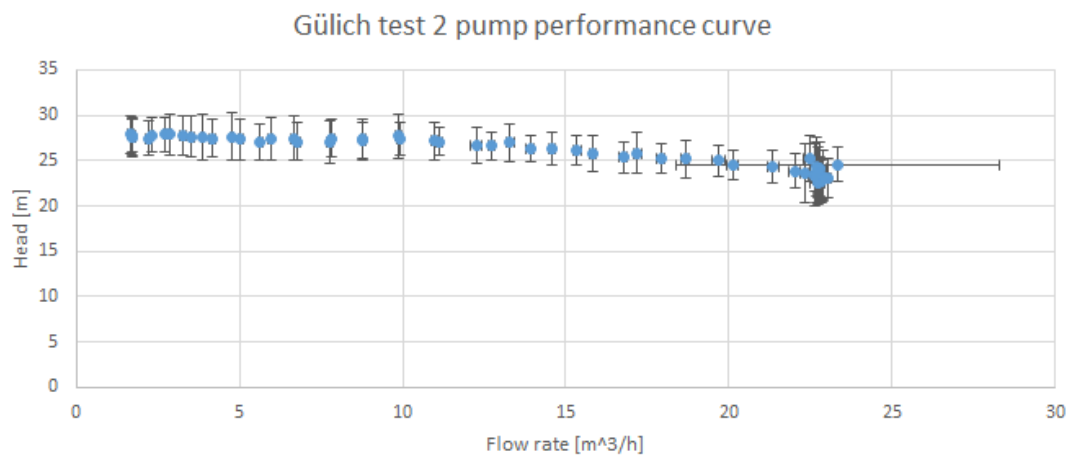


Figure F.2: Gülich impeller test 2

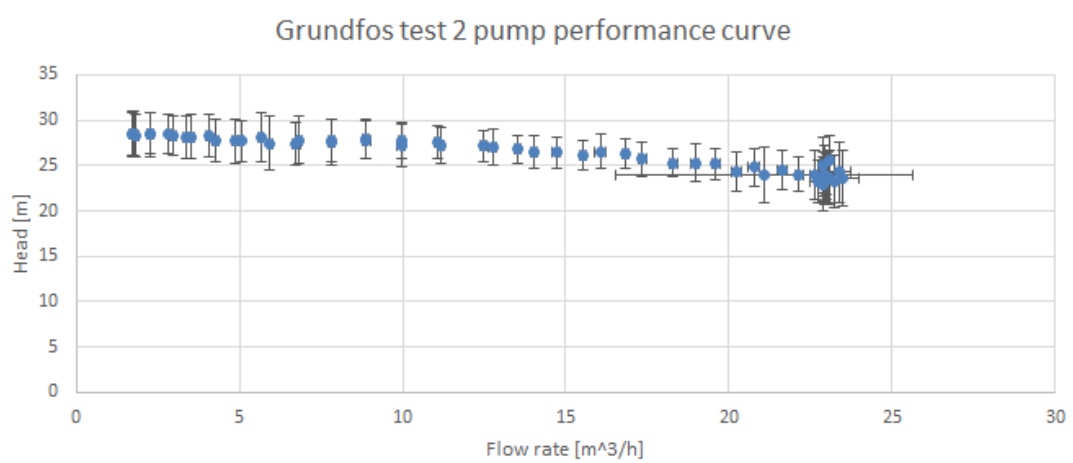


Figure F.3: Grundfos impeller test 2

## G. CD CONTENT

*ImpellerDesign.pdf* is the report (This includes the *hyperref* function)

### Calculations

- *BladeDesign.m* is the MATLAB script that calculates the blade coordinates.
- *ImpellerDesignBohl.m* calculation model of the Bohl impeller.
- *ImpellerDesignGulich.m* calculation model of the Gülich impeller.

### Impeller drawings

- *ImpellerBohl* contains a 3D sketch of the Bohl impeller.
- *ImpellerGulich* contains a 3D sketch of the Gülich impeller.

### Impeller figures

- *Bohlimpeller.png* is a figure of the finished Bohl impeller.
- *Gulichimpeller.png* is a figure of the finished Gülich impeller.

### Impeller experiments

- *Bohl impeller* contains experimental data of the Bohl impeller.
- *Gülich impeller* contains experimental data of the Gülich impeller.
- *Grundfos impeller* contains experimental data of the Grundfos impeller.
- *Comparing* contains experimental data of the Bohl and Gülich impeller compared with the Grundfos impeller.